



HAL
open science

NHC Core Phosponium Ylide-based Palladium(II) Pincer Complexes: The Second Ylide Extremity Makes the Difference

Rachid Taakili, Cécile Barthes, Amel Goëffon, Christine Lepetit, Carine Guyard-Duhayon, Dmitry A. Valyaev, Yves Canac

► **To cite this version:**

Rachid Taakili, Cécile Barthes, Amel Goëffon, Christine Lepetit, Carine Guyard-Duhayon, et al.. NHC Core Phosponium Ylide-based Palladium(II) Pincer Complexes: The Second Ylide Extremity Makes the Difference. *Inorganic Chemistry*, American Chemical Society, 2020, 59 (10), pp.7082-7096. 10.1021/acs.inorgchem.0c00561 . hal-02612432

HAL Id: hal-02612432

<https://hal.archives-ouvertes.fr/hal-02612432>

Submitted on 6 Nov 2020

HAL is a multi-disciplinary open access archive for the deposit and dissemination of scientific research documents, whether they are published or not. The documents may come from teaching and research institutions in France or abroad, or from public or private research centers.

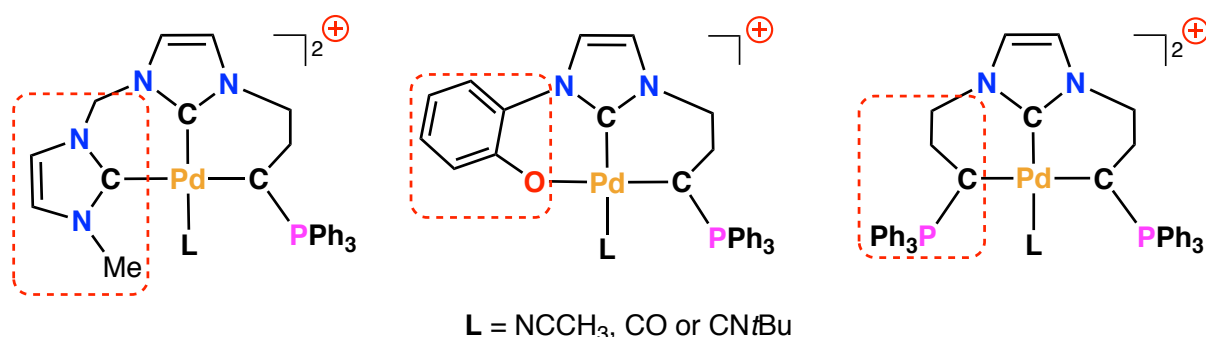
L'archive ouverte pluridisciplinaire **HAL**, est destinée au dépôt et à la diffusion de documents scientifiques de niveau recherche, publiés ou non, émanant des établissements d'enseignement et de recherche français ou étrangers, des laboratoires publics ou privés.

NHC Core Phosponium Ylide-Based Palladium(II) Pincer Complexes: The Second Ylide Extremity Makes the Difference

Rachid Taakili, Cécile Barthes, Amel Goëffon, Christine Lepetit,
Carine Duhayon, Dmitry A. Valyaev, Yves Canac*

LCC–CNRS, Université de Toulouse, CNRS, 205 route de Narbonne 31077 Toulouse cedex
4, France. E-mail: yves.canac@lcc-toulouse.fr

GRAPHICAL ABSTRACT:

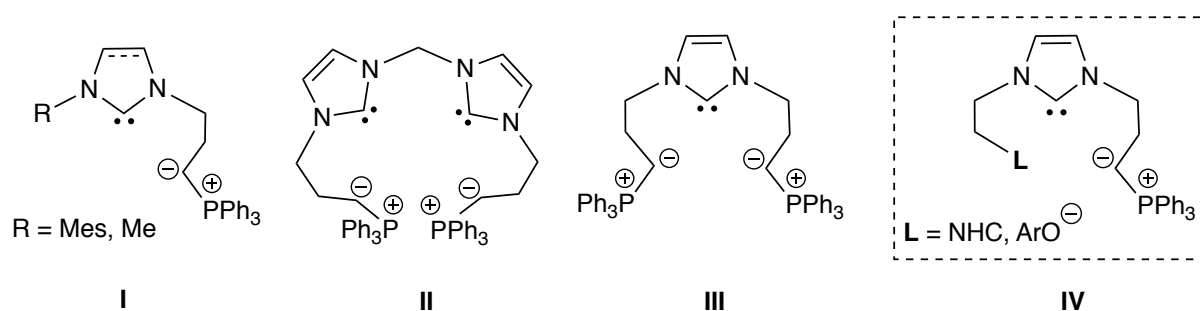


ABSTRACT: The coordinating properties of NHC (A), phenolate (B) and phosphonium ylide (C) moieties have been investigated systematically through the preparation of a family of NHC, phosphonium ylide-based pincer ligands where the third donor extremity can be either a NHC, a phenolate or a phosphonium ylide. The overall donor character of such ligands $[\text{NHC}(\text{A}_a\text{B}_b\text{C}_c)]$ ($a + b + c = 2$) has been analyzed by comparison of the MOs (energy and shape), oxidation potentials (E_p^{ox}), and IR ν_{CO} and ν_{CN} stretching frequencies of their isostructural pincer Pd(II) complexes $[\text{NHC}(\text{A}_a\text{B}_b\text{C}_c)\text{PdL}][\text{OTf}]$ ($L = \text{NCCH}_3, \text{CO} \text{ or } \text{CN}t\text{Bu}$). The three categories of pincer complexes based on phosphonium ylides were easily obtained by acidic treatment of their highly stable *ortho*-metallated Pd(II) precursors prepared in a single step from readily available N-phosponio-substituted imidazolium salts. Analysis of IR data indicated that NHC and phenolate ligands have a similar donor character but which remains lower than that of the phosphonium ylide. The impact on catalytic performance of the incorporation of a second strongly donating phosphonium ylide into the ligand architecture has been illustrated in the Pd-catalyzed allylation of aldehydes.

Keywords: Allylation, carbon ligand, NHC, palladium, phosphonium ylide, phenolate, pincer.

1. INTRODUCTION

The isolation of the first stable singlet carbenes¹ proved to be a trigger in the minds of chemists, leading in a short time to remarkable advances in various fields, such as organometallic chemistry, functional materials and homogeneous catalysis.² From there, considerable efforts have been provided to introduce structural diversity and carbene ligands have become unavoidable surpassing in some applications their illustrious predecessors based on group 15 elements.³ Like carbenes, onium ylides and related species which are charge-neutral in their free state and act as strong σ -donors with weak π -acceptor ability,⁴ have experienced a revival of interest confirming their potential as Lewis bases in main group⁵ and coordination chemistry.⁶ Phosphonium ylides, the most exemplified representatives of this family, differ in the hybridization state of the coordinating atom with respect to NHCs - Csp^3 -type vs. Csp^2 -type -, thus positioning themselves as a complementary class of carbon ligands. Based on the preparation of an isostructural series of Rh(I) dicarbonyl complexes, it was experimentally⁷ and theoretically⁸ demonstrated that phosphonium ylides behave as stronger donor ligands than NHCs. However, while NHCs promote a large number of transition-metal-catalyzed reactions,⁹ the catalytic applications of phosphonium ylides remained in their infancy.¹⁰ Following pioneering reports in the field aimed at developing catalytically activated ylide-based metal systems,¹¹ NHC and phosphonium ylide donor moieties were recently associated by a flexible C_3 -propyl linker in the bi- (**I**),¹² tetradente (**II**),¹³ and in the pincer series (**III**)¹⁴ forming extremely electron-rich metal complexes, thanks to the design of a general synthetic strategy (Scheme 1).¹⁵ As striking fact, the C,C,C -NHC, diphosphonium bis(ylide)ligand **III** of LX_2 -type was shown to efficiently stabilize a Pd(II) carbonyl complex¹⁴ whose examples of this type remain scarce due to easy Pd-CO dissociation.¹⁶



Scheme 1. Representation of recently reported chelating NHC, phosphonium ylide ligands **I–III**^{12–14} and related targeted pincer systems of type **IV**.

These experimental advances encourage us to undertake a precise study on the electronic features of this type of carbon-based ligands and their pincer complexes in order to consider catalytic applications. The challenge is envisaged on the basis of the preparation of a test family of phosphonium ylide-based Pd(II) pincer complexes **IV** in which a globally neutral phosphonium ylide (1- e^- donor (X-type)) of the symmetrical NHC, bis(phosphonium ylide) ligand **III** is strictly replaced either by a neutral NHC (2- e^- donor (L-type)) or by an anionic phenolate (1- e^- donor (X-type)) (Scheme 1).¹⁷ The objective is to carry out this comparative study while preserving the overall architecture of the pincer complexes defined by the NHC core and the two fused six-membered palladacycles resulting from the coordination of the three donor ends. Furthermore, the meridional tridentate coordination mode of pincer ligands leaves generally an open coordination site,¹⁸ which should be beneficial for the introduction of a carbonyl or an isocyanide co-ligand able to act as an electronic probe to evaluate the overall σ -donating *vs.* π -accepting properties of the targeted ligands.^{14,19}

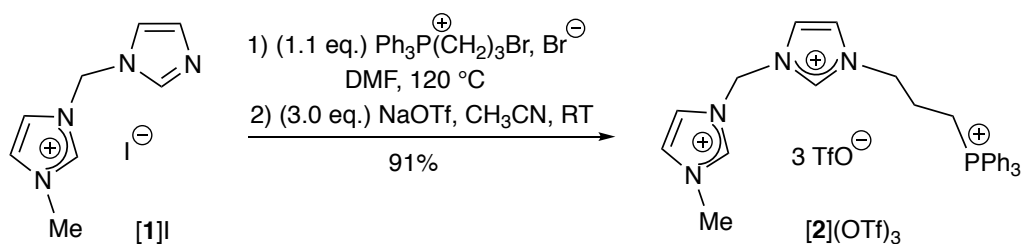
The present contribution addresses the preparation, the coordinating behavior towards Pd(II) centers, and the catalytic properties of NHC, phosphonium ylide-based pincer ligands of type **III–IV** (Scheme 1), providing thus a systematic comparison of three complementary coordinating functional groups (*ca.* phosphonium ylide, NHC and phenolate) of broad interest in organometallic chemistry and homogeneous catalysis.

2. RESULTS AND DISCUSSION

2.1 Synthesis and NMR characterization of NHC, phosphonium ylide-based pincer pre-ligands and their Pd(II) complexes

2.1.1 Bis(NHC), phosphonium ylide series

The first target was a palladium complex of the pincer ligand of type **IV** where the peripheral coordinating extremity L is a N-bonded N-methylimidazolylidene (Scheme 1, *right*). For this purpose, the N-phosphonio-substituted bis(imidazolium) salt **[2]**(OTf)₃ was readily prepared in 91% overall yield by treating 3-((1H-imidazol-1-yl)-methyl)-1-methyl-1H-imidazol-3-ium iodide **[1]**I²⁰ with 1.1 equiv. of (3-bromopropyl)triphenylphosphonium bromide in DMF at 120 °C followed by anion metathesis with NaOTf in CH₃CN (Scheme 2).

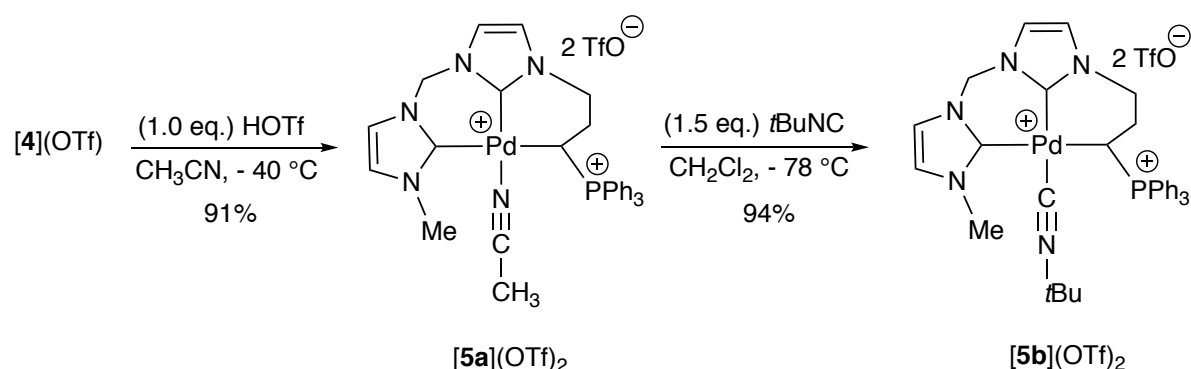


Scheme 2. Preparation of N - $[(\text{CH}_2)_3\text{PPh}_3]^+$ substituted bis(imidazolium) salt $[\mathbf{2}](\text{OTf})_3$ from $[\mathbf{1}]\text{I}$.

The ^{31}P NMR spectrum of $[\mathbf{2}](\text{OTf})_3$ displayed a single signal at δ_{P} 25.0 ppm in the normal range for phosphonium salts.²¹ The two imidazolium protons of $[\mathbf{2}](\text{OTf})_3$ were evidenced by the characteristic low field signals at δ_{H} 9.10 and 9.31 ppm in the ^1H NMR spectrum. On the basis of recent results¹²⁻¹⁴ where a difference in acidity between the H-atoms of imidazolium and alkyl phosphonium moieties was observed,²² the complexation of $[\mathbf{2}](\text{OTf})_3$ was envisioned through a sequential strategy. Treatment of pre-ligand $[\mathbf{2}](\text{OTf})_3$ with a stoichiometric amount of $[\text{PdCl}_2(\text{MeCN})_2]$ in the presence of Et_3N in CH_3CN cleanly afforded the N -phosphonio-bis(NHC) PdCl_2 complex $[\mathbf{3}](\text{OTf})$ in 75% yield (Scheme 3). The formation of complex $[\mathbf{3}](\text{OTf})$ was clearly indicated by ^1H NMR spectroscopy showing the disappearance of the C–H imidazolium signals of $[\mathbf{2}](\text{OTf})_3$. The unchanged environment of the phosphonium moieties in Pd complex $[\mathbf{3}](\text{OTf})$ compared to $[\mathbf{2}](\text{OTf})_3$ was demonstrated by the similarity of their ^{31}P NMR chemical shifts ($[\mathbf{2}](\text{OTf})_3$: δ_{P} 25.0 ppm; $[\mathbf{3}](\text{OTf})$: δ_{P} 23.6 ppm). In the ^{13}C NMR spectra, the N_2C –Pd carbon atoms of NHC complex $[\mathbf{3}](\text{OTf})$ (δ_{C} 158.5 and 159.0 ppm) were typically found to be deshielded with respect to the N_2CH carbon atoms of precursor $[\mathbf{2}](\text{OTf})_3$ (δ_{C} 138.6 and 138.8 ppm). The cationic character of Pd complex $[\mathbf{3}](\text{OTf})$ was confirmed by ESI mass spectroscopy ($\mathbf{3}^+$: m/z 642.9 $[\text{M} - \text{OTf}]^+$).

According to the conditions developed in the NHC, bis(ylide) series,¹⁴ the PdCl_2 complex $[\mathbf{3}](\text{OTf})$ was treated with 3 equiv. of Cs_2CO_3 in CH_3CN at 60 °C.²³ The present system allowed thus the selective formation of the *ortho*-metallated bis(NHC), phosphonium ylide Pd complex $[\mathbf{4}](\text{OTf})$ in 94% yield. Gratifyingly, the latter could be obtained directly in 69% yield by reacting the dicationic salt $[\mathbf{2}](\text{OTf})_3$ with PdCl_2 in the presence of 5 equiv. of Cs_2CO_3 in CH_3CN at 60 °C (Scheme 3). The *ortho*-metallated complex $[\mathbf{4}](\text{OTf})$ available on a gram scale appeared to be highly stable in air both in the solid state and in solution, and insensitive to moisture.

coordinated CH₃CN molecule as indicated by the corresponding single resonance (δ_C 2.2 ppm).



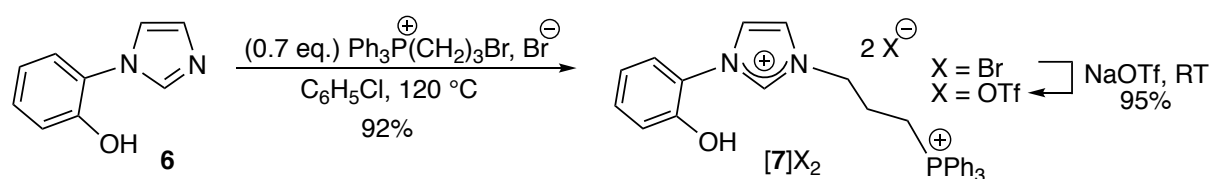
Scheme 4. Synthesis of the bis(NHC), phosphonium ylide Pd(II) pincer complex **[5a](OTf)₂** from **[4](OTf)**, and exchange reaction at the Pd center of **[5a](OTf)₂** with *t*-butyl isocyanide with formation of the pincer complex **[5b](OTf)₂**.

To evaluate the overall donating properties of the bis(NHC) ligand of complex **[5a](OTf)₂**, the substitution of the CH₃CN co-ligand by the stronger σ -donating *t*-butyl isocyanide able to act as a valuable IR probe was envisioned. The exchange reaction at the Pd atom was realized in CH₂Cl₂ at -78 °C affording the targeted isocyanide adduct **[5b](OTf)₂** in 94% yield (Scheme 4). While the ³¹P NMR spectrum remained almost unchanged (δ_P 35.0 ppm; **[5a](OTf)₂**: δ_P 33.9 ppm), the coordination of the isocyanide was evidenced by the ¹H and ¹³C NMR resonances of the *t*-Bu group at δ_H 1.06 ppm, and δ_C 29.5 and 59.7 ppm, respectively.²⁴ The $\nu_{C\equiv N}$ IR band observed at 2206 cm⁻¹ in CH₂Cl₂ confirmed the presence of the [Pd-C \equiv N-*t*Bu] sequence in complex **[5b](OTf)₂**.²⁵ Having in mind the thermal stability of a Pd-CO complex of the bis(ylide) ligand (**[12c](OTf)₂**, Table 1),¹⁴ CO gas was bubbled through a solution of **[5a](OTf)₂** in CH₂Cl₂. However whatever the experimental conditions used (CO pressure, T °C and reaction time), ³¹P NMR monitoring indicated only the presence of **[5a](OTf)₂**, the bis(NHC), ylide ligand being therefore not capable to stabilize a Pd-CO adduct, probably due to its insufficient donor character.

2.1.2 NHC, phenolate, phosphonium ylide series

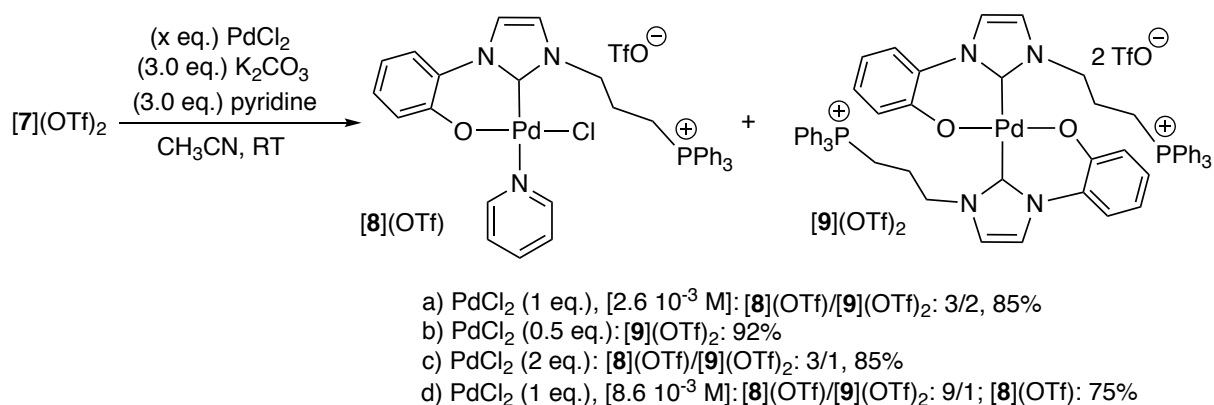
Access to the third representative of the family based on a *C,C,O*- pincer ligand where the central NHC is N-substituted by a C-bonded phenolate and a C-bonded phosphonium ylide fragments, was envisioned from 1-(2-hydroxyphenyl)imidazole **6**.²⁶ Similar reactivity pattern to that observed previously could be obtained by reacting imidazole **6** with (3-bromopropyl)-

triphenylphosphonium bromide in C₆H₅Cl at 120 °C. The corresponding N-phosphonio substituted imidazolium salt [7]Br₂ was isolated in 92% yield (Scheme 5). By an anionic metathesis reaction carried out with NaOTf in CH₂Cl₂, the imidazolium [7]Br₂ was transformed into its triflate salt [7](OTf)₂ more soluble in conventional organic solvents with a yield of 95%. The presence of a singlet at δ_p 23.9–24.3 ppm in the ³¹P NMR spectra for the pending phosphonium and a singlet at δ_H 9.2–9.9 ppm for the imidazolium core in the ¹H NMR spectra are in agreement with the dicationic character of salts [7]X₂ (X = Br, OTf).



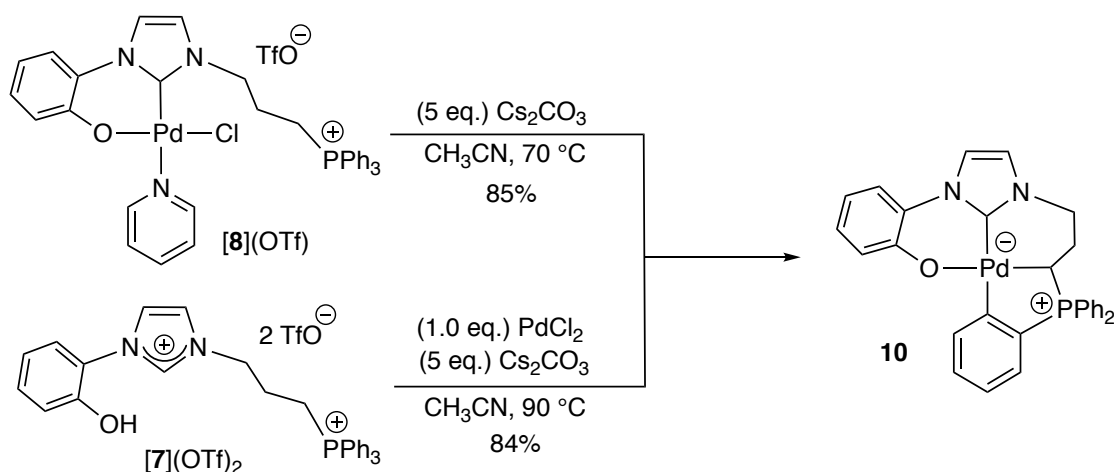
Scheme 5. Preparation of *N*-[(CH₂)₃PPh₃]⁺ substituted imidazolium salts [7]X₂ (X = Br, OTf) from **6**.

Anticipating that [7](OTf)₂ should behave like an LX₂-type ligand in the Green formalism,¹⁷ its coordination was achieved by adding a stoichiometric amount of PdCl₂ in the presence of the K₂CO₃/pyridine system in CH₃CN.²⁷ These specific conditions produce a 3/2 mixture of Pd(II) complexes [8](OTf) and [9](OTf)₂ in 85% overall yield differentiating by the ligand/metal ratio (Scheme 6). Their formation was clearly indicated by ¹H NMR spectroscopy which shown the disappearance of the characteristic imidazolium signal of precursor [7](OTf)₂. In both cases, the absence of the ¹H NMR signal for the hydroxyl group suggests the concomitant O-coordination of the phenolate moiety. In [8](OTf), the linkage of the pyridine to the Pd center was clearly indicated by the presence of three ¹H NMR resonances at δ_H 8.86, 7.99 and 7.55 ppm in the aromatic region. Noteworthy, addition of 0.5 equiv. of PdCl₂ to [7](OTf)₂ in the presence of K₂CO₃ resulted in the unique formation of the bis(NHC), bis(phenolate) Pd complex [9](OTf)₂, isolated in 92% yield. Setting the ratio [7](OTf)₂/Pd to 1/2 afforded a better selectivity ([8](OTf)/[9](OTf)₂: 3/1, overall yield 85%). However to significantly improve the selectivity, more dilute conditions were needed leading with the initial stoichiometry ([7](OTf)₂/Pd:1/1) to the complex [8](OTf) in a 75% yield with a ratio [8](OTf)/[9](OTf)₂ of 9/1 (Scheme 6).



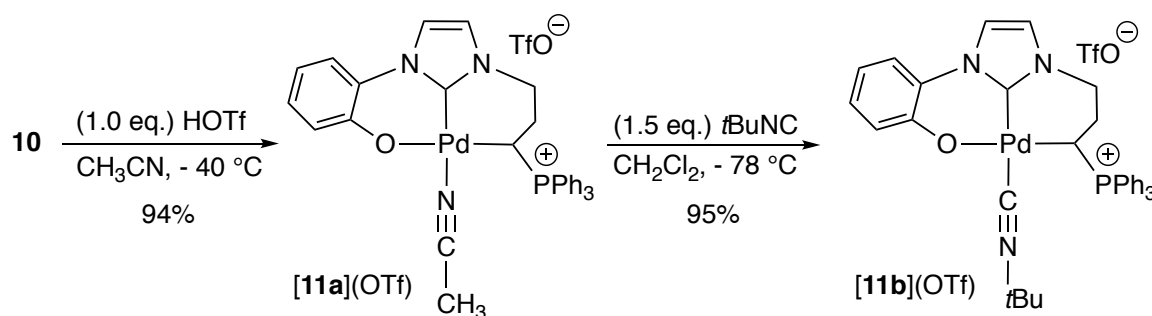
Scheme 6. Synthesis of N-phosponio-NHC, phenolate Pd(II) complex [8](OTf) and bis(N-phosponio-NHC, phenolate) Pd(II) complex [9](OTf)₂ from [7](OTf)₂.

Thanks to the optimized conditions developed in the previous series, the complex [8](OTf) was readily converted in a 85% yield into its *ortho*-metallated form **10** upon addition of an excess of Cs₂CO₃ in CH₃CN at 70 °C (Scheme 7).²³ The *ortho*-metallated complex **10** could be also directly prepared from the pre-ligand [7](OTf)₂ in a 84% isolated yield following an one-pot strategy. The high stability observed with regard to air and moisture, as well as the possibility of preparing it on a gram scale make complex **10** a precursor of choice for the ensuing pincer. In the complex **10**, the coordination of the CH ylide moiety was unveiled by ³¹P, ¹H and ¹³C NMR spectroscopy, especially on the basis on the high-field ¹³C NMR doublet at δ_{CH} 13.8 ppm with a ¹J_{CP} coupling constant of 40.2 Hz. The *ortho*-metallated fragment is confirmed by the presence of corresponding strongly deshielded ¹³C NMR signals at δ_C 182.2 ppm (d, ²J_{CP} = 37.2 Hz) and δ_C 137.1 ppm (d, ¹J_{CP} = 119.7 Hz).



Scheme 7. Synthesis of the NHC, phenolate, phosphonium ylide Pd(II) complex **10** from N-phosponio-NHC, phenolate Pd(II) complex [8](OTf) or imidazolium salt [7](OTf)₂.

To evaluate the donating properties of the *C,C,O*- pincer ligand of interest, the same sequential strategy as that developed in the bis(NHC) series was targeted. Thanks to two selective transformations, the pincer Pd-adducts **[11a]**(OTf) and **[11b]**(OTf) were formed in high yields from **10** by acidic cleavage of the *Csp*²-Pd bond of the phenylated ring followed by nucleophilic displacement of the incoming CH₃CN co-ligand by *t*BuNC (Scheme 8). Upon exchange at the Pd(II) center (pyridine vs. CH₃CN vs. *t*BuNC), the ³¹P NMR chemical shifts remained essentially unchanged with the presence of a deshielded singlet (**10**: δ_P = 33.8 ppm; **[11a]**(OTf): δ_P = 29.0 ppm; **[11b]**(OTf): δ_P = 31.8 ppm). In all cases, ¹³C NMR spectra are characterized by the occurrence of a doublet at low field for the linked ylide moiety (**10**: δ_{CH} = 13.8 ppm (¹J_{CP} = 40.2 Hz); **[11a]**(OTf): δ_{CH} = 5.7 ppm (¹J_{CP} = 32.2 Hz); **[11b]**(OTf): δ_{CH} = 3.3 ppm (¹J_{CP} = 32.7 Hz)). While in the complex **[11a]**(OTf), the presence of coordinated CH₃CN was confirmed by the corresponding ¹³C NMR resonance (δ_C 2.2 ppm in CD₂Cl₂), in **[11b]**(OTf) the coordination of the isocyanide was evidenced by the typical IR ν_{CN} band at 2207 cm⁻¹ in CH₂Cl₂. As in the bis(NHC), ylide series, no formation of Pd-CO adduct was observed when the complex **[11a]**(OTf) was treated with CO gas in CH₂Cl₂.



Scheme 8. Synthesis of NHC, phenolate, phosphonium ylide Pd(II) pincer complexes **[11a]**(OTf) and **[11b]**(OTf) from **10** by successive additions of HOTf and *t*BuNC.

2.2 Solid-state structural studies

Single crystal X-ray diffraction studies allowed us to establish the solid-state structures of the imidazolium salt **[7]**Br₂, and of the corresponding Pd complexes **[8]**(OTf) and **[9]**(OTf)₂ (Figure 1).²⁸ In both complexes, the Pd(II) atom resides in a square-planar environment. However, while in the complex **[8]**(OTf), the position *trans* relative to the NHC is occupied by the pyridine, in the centro-symmetric complex **[9]**(OTf)₂, the bidentate chelating *C,O*-ligand binds to the Pd atom in a *trans* fashion. Noteworthy, the N₂C-Pd bond distances in **[9]**(OTf)₂ are slightly longer than in **[8]**(OTf) (**[8]**(OTf): C1-Pd1 = 1.965(3) Å; **[9]**(OTf)₂: C1-Pd1 = 2.011(5) Å), a difference which may be tentatively attributed to the existence of

steric and electrostatic constraints between the facing cationic ligands in complex **[9](OTf)₂**, the two triarylphosphoniums being on either side of the coordination Pd plane.

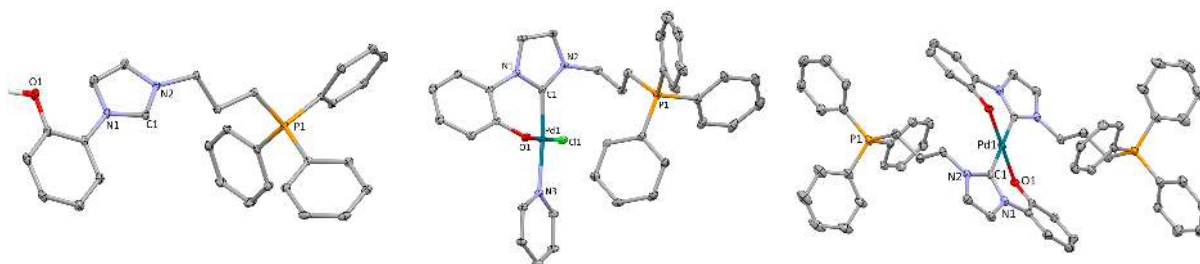


Figure 1. Perspective views of the cationic part of N-phosponio-imidazolium salt **[7]Br₂** (*left*), N-phosponio-substituted NHC Pd complex **[8](OTf)** (*middle*), and bis(N-phosponio-substituted NHC) Pd complex **[9](OTf)₂** (*right*) with thermal ellipsoids drawn at the 30% probability level. The H atoms are omitted for clarity. Selected bond lengths [Å] and angles [°]: **[7]Br₂**: C1–N1 = 1.3394(18); C1–N2 = 1.3308(19); N1–C1–N2 = 108.47(13); **[8](OTf)**: C1–N1 = 1.359(3); C1–N2 = 1.344(3); C1–Pd1 = 1.965(3); O1–Pd1 = 2.0133(18); C11–Pd1 = 2.3162(6); N3–Pd1 = 2.127(2); N1–C1–N2 = 105.4(2); C1–Pd1–N3 = 172.79(10); O1–Pd1–C11 = 178.42(6); C1–Pd1–O1 = 84.21(9); C1–Pd1–C11 = 94.44(8); **[9](OTf)₂**: C1–N1 = 1.361(7); C1–N2 = 1.353(7); C1–Pd1 = 2.011(5); O1–Pd1 = 2.001(3); N1–C1–N2 = 104.0(4); C1–Pd1–C1 = 179.994; O1–Pd1–O1 = 179.994; C1–Pd1–O1 = 93.92(17).

By marked contrast with the bis(ylide) series where single crystals of the *ortho*-metallated form could not be obtained,¹⁴ the exact structure of related Pd complexes **[4](OTf)** and **10** was established by an X-ray diffraction analysis of single yellow crystals (Figure 2).²⁸ In complex **[4](OTf)**, the Pd(II) atom resides in a slightly distorted square-planar environment where the coordination plane is defined by four carbon donor extremities, namely the C1, C7, C11, and C13 atoms of the two NHCs, the phosphonium ylide and the *ortho*-phenylated moieties, respectively (Figure 2, *left*). The two *cis*-NHC fragments are positioned in respective *trans* position of the ylide and aryl groups with corresponding angles, which slightly deviate from ideal values (C1–Pd1–C11 = 173.95(18)°; C7–Pd1–C13 = 172.95(19)°). The NHC–Pd bond distances (C1–Pd1 = 2.018(2) Å; C7–Pd1 = 2.003(5) Å) fall within the range of related (NHC) Pd(II) complexes, being classically shorter than the ylide–Pd bond distance (C11–Pd1 = 2.112(5) Å) in agreement with their respective hybridization state (*Csp²* vs. *Csp³*).¹⁴ The two fused six-membered palladacycles adopt a boat-like conformation with the sterically hindered tetrahedral phosphonium located in equatorial position while being an integral part of the *ortho*-metallated five-membered ring.

The *ortho*-metallated complex **10** presents a zwitterionic *C,C,C,O*-chelated structure, where the phosphonium positive charge is compensated by a palladate negative charge (figure 2, *right*). To accommodate a square planar geometry for the Pd(II) atom, the molecule is globally planar where only the phosphonium center and a CH₂ group of the propyl chain deviate from the planarity. The NHC core is located in *trans* position relative to the phenylated ring while the phenolate extremity is *trans* with respect to the ylide fragment (C1–Pd1–C13 = 172.71(4)°; C6–Pd1–O1 = 177.95(3)°). According to their respective hybridization state, the coordination bonds around the Pd center lie in the normal range for such donor groups (NHC: C1–Pd1 = 2.0107(10) Å; RC₆H₄O[−]: O1–Pd1 = 2.0411(8) Å; Ph₃P⁺CHR[−]: C6–Pd1 = 2.0593(9) Å; RC₆H₄[−]: C13–Pd1 = 2.0366(9) Å). The tau parameter (τ_4) which reflects the deviation from a square planar geometry was calculated in both cases.²⁹ The values found, respectively 0.091 and 0.065 in complexes [4](OTf) and **10**, close to 0, indicate a small deviation from a square planar geometry despite the presence of constrained structures.

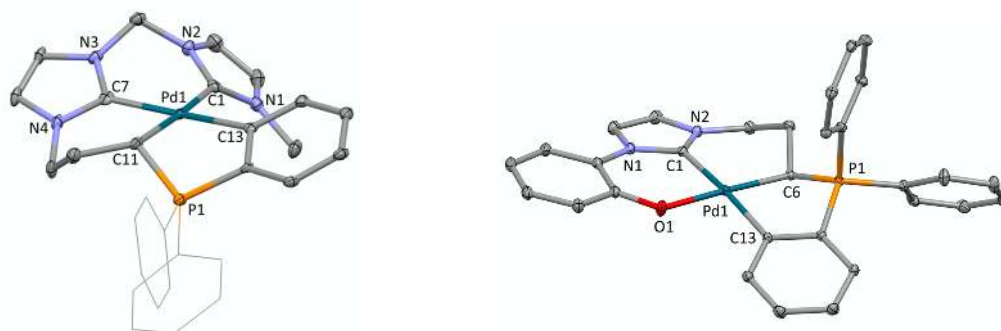


Figure 2. Perspective views of bis(NHC), phosphonium ylide Pd complex [4](OTf) (*left*), and NHC, phenolate, phosphonium ylide Pd complex **10** (*right*) with thermal ellipsoids drawn at the 30% probability level. The H atoms are omitted and phenyl rings are presented as wireframe for clarity in the case of [4](OTf). Selected bond lengths [Å] and angles [°]: [4](OTf): C1–N1 = 1.349(6); C1–N2 = 1.366(6); C7–N3 = 1.355(6); C7–N4 = 1.333(7); C1–Pd1 = 2.043(5); C7–Pd1 = 2.003(5); C11–Pd1 = 2.112(5); C13–Pd1 = 2.065(5); N1–C1–N2 = 103.0(4); N3–C7–N4 = 104.6(4); C1–Pd1–C11 = 173.95(18); C7–Pd1–C13 = 172.95(19); C1–Pd1–C7 = 85.75(19); C7–Pd1–C11 = 88.42(19); C11–Pd1–C13 = 85.71(18). **10**: C1–N1 = 1.3710(12); C1–N2 = 1.3522(13); P1–C6 = 1.7765(9); C1–Pd1 = 2.0107(10); O1–Pd1 = 2.0411(8); C6–Pd1 = 2.0593(9); C13–Pd1 = 2.0366(9); N1–C1–N2 = 104.85(8); C1–Pd1–C13 = 172.71(4); C6–Pd1–O1 = 177.95(3); C1–Pd1–O1 = 89.84(4); C6–Pd1–C13 = 87.77(4).

2.3 IR spectroscopy, cyclic voltammetry and theoretical studies of a series of Pd(II) pincer complexes.

The IR ν_{CN} frequency values of Pd complexes **[5b]**(OTf)₂ ($\nu_{\text{C}\equiv\text{N}}$ 2206 cm⁻¹) and **[11b]**(OTf) ($\nu_{\text{C}\equiv\text{N}}$ 2207 cm⁻¹) indicate that the *C,C,C*-bis(NHC), phosphonium ylide and *C,C,O*-NHC, phenolate, phosphonium ylide ligands have a similar donor character. However, these values which occur at higher frequency than that of the Pd–CN*t*Bu complex of the bis(ylide), NHC ligand (**[12b]**(OTf)₂: $\nu_{\text{C}\equiv\text{N}}$ 2194 cm⁻¹ in CH₂Cl₂)¹⁴ suggest also that substitution of a NHC or a phenolate for a phosphonium ylide increase significantly the donor character of corresponding pincer ligands (Table 1). This trend is in line with previous studies conducted on an isoelectronic family of *C,C*-chelating [*o*-C₆H₄A_aB_bRh(CO)₂][OTf] complexes (A = NHC; B = Ph₂P⁺CH₂).⁷⁻⁸

The IR ν_{CN} and ν_{CO} frequencies of cationic Pd complexes **5**²⁺, **11**⁺ and **12**²⁺ were calculated at the DFT level and compared with the experimental values.³⁰ A good agreement between experimental and calculated ν_{CN} values was obtained with a constant gap of Δ (calcd-exp) \approx 8–9 cm⁻¹. Both calculated ν_{CN} and ν_{CO} stretching frequencies confirm the strong donor character of phosphonium ylides as illustrated with the Pd–CO complex only observed experimentally in the case of the bis(ylide) ligand.¹⁴ Along the two series, calculated values agree with the experimental trend, namely the highest donating properties of the pincer ligand in complex **12**²⁺ and similar electron-donating properties for the ligands in complexes **5**²⁺ and **11**⁺.

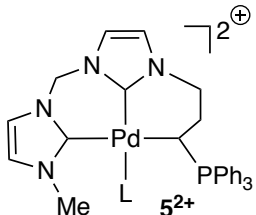
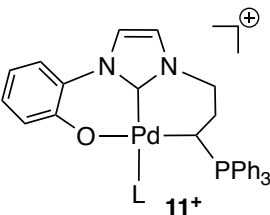
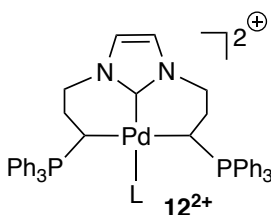
			
a: L = NCCH ₃			
b: L = CN <i>t</i> Bu			
c: L = CO			
ν_{CN} (exp) ^a	5b ²⁺ : 2206	11b ⁺ : 2207	12b ²⁺ : 2194
ν_{CN} (calcd) ^b	5b ²⁺ : 2215	11b ⁺ : 2215	12b ²⁺ : 2207 2199 2203 (av.) ^c
Δ (calcd-exp)	9	8	9
ν_{CO} (exp) ^a	—	—	12c ²⁺ : 2114
ν_{CO} (calcd) ^b	5c ²⁺ : 2095	11c ⁺ : 2097	12c ²⁺ : 2076 2079 2077.5 (av.) ^c
E_p^{ox} ^d	5a ²⁺ : 1.9 (1.5) ^e	11a ⁺ : 2.1 (1.8) ^e	12a ²⁺ : 1.6 (1.2) ^e

Table 1. Experimental and calculated IR ν_{CO} and ν_{CN} stretching frequencies (cm⁻¹), and E_p^{ox} (V) for the cationic complexes **5**²⁺, **11**⁺ and **12**²⁺.^a IR frequency values measured in CH₂Cl₂.^b

Calculations were performed at the PBE-D3/6-31G**/LANL2DZ*(Pd) level.^c Complexes **12**²⁺ exist as a mixture of *meso*- and *dl*-diastereoisomers.^{14 d} E_{p}^{ox} values (V) are given with respect to SCE.^e The values between brackets correspond to the E_{p}^{ox} (V) of related *ortho*-metallated forms.

The near-frontier orbitals of Pd pincer complexes **5**²⁺, **11**⁺ and **12**²⁺ were investigated in the isocyanide and carbonyl series.³¹ The HOMOs of Pd–CN*t*Bu and Pd–CO adducts are depicted in Figure 3. In the isocyanide series, the HOMOs of carbon-based Pd complexes **5b**²⁺ and **12b**²⁺ involve a strong contribution of the orbitals of the Pd center and the carbon atom of the highly donating phosphonium ylide, accounting for the Csp^3 –Pd σ bond (Figure 3, top). Consistently with the respective electron-richness of pincer ligands, the replacement of a NHC by a phosphonium ylide induces a shift of the HOMO towards higher energy (**5b**²⁺: –10.9 eV; **12b**²⁺: –10.1 eV). This variation is consistent with the formal charge at the palladium atom: +1 in **5b**²⁺, 0 in **12b**²⁺, the oxidation state of the metal (Pd(II)) and the overall charge of the complexes (+2) remaining the same. As the shape of HOMOs may be related to the ligand-metal interaction, the near-frontier MO energy levels of complexes **5b**²⁺ and **12b**²⁺ can be tentatively correlated with the electronic properties of corresponding C,C,C-pincer ligands following thus the same trend than IR ν_{CN} and ν_{CO} stretching frequencies. In contrast in complex **11b**⁺, the HOMO is strongly localized on the π -system and the oxygen atom lone pair of the phenolate donor with a negligible contribution of the Pd atom. The MOs exhibiting a significant contribution of the Pd and the ylide fragments are shifted much deeper in energy, as illustrated by the energies of HOMO–15 (–9.9 eV) and HOMO–16 (–10.0 eV). The MOs and in particular the HOMO (*ca.* –6.6 eV) lie significantly higher in energy compared to the carbon-based systems **5b**²⁺ and **12b**²⁺. This difference can be assigned to the different overall charge [**11b**⁺ (+1), **5b**²⁺ and **12b**²⁺ (+2)]. Since the HOMO does not properly account for the ligand-metal interaction in complex **11b**⁺, its energy cannot be directly related to the electronic properties of the ligand and therefore to the ν_{CN} and ν_{CO} frequency values. In terms of relative energy of HOMOs, the same general trend was found in the Pd–CO adducts (HOMO energy for **5c**²⁺: –11.2 eV; **11c**⁺: –7.0 eV; **12c**²⁺: –10.5 eV) (Figure 3, bottom). However, while the HOMOs remained mainly localized on the phenolate moiety and on the Pd and ylidic carbon atoms respectively in complexes **11c**⁺ and **12c**²⁺, in the case of the bis(NHC) Pd complex **5c**²⁺, the HOMO is strongly localized on a P⁺-phenyl substituent on the way to the corresponding *ortho*-metallated form.

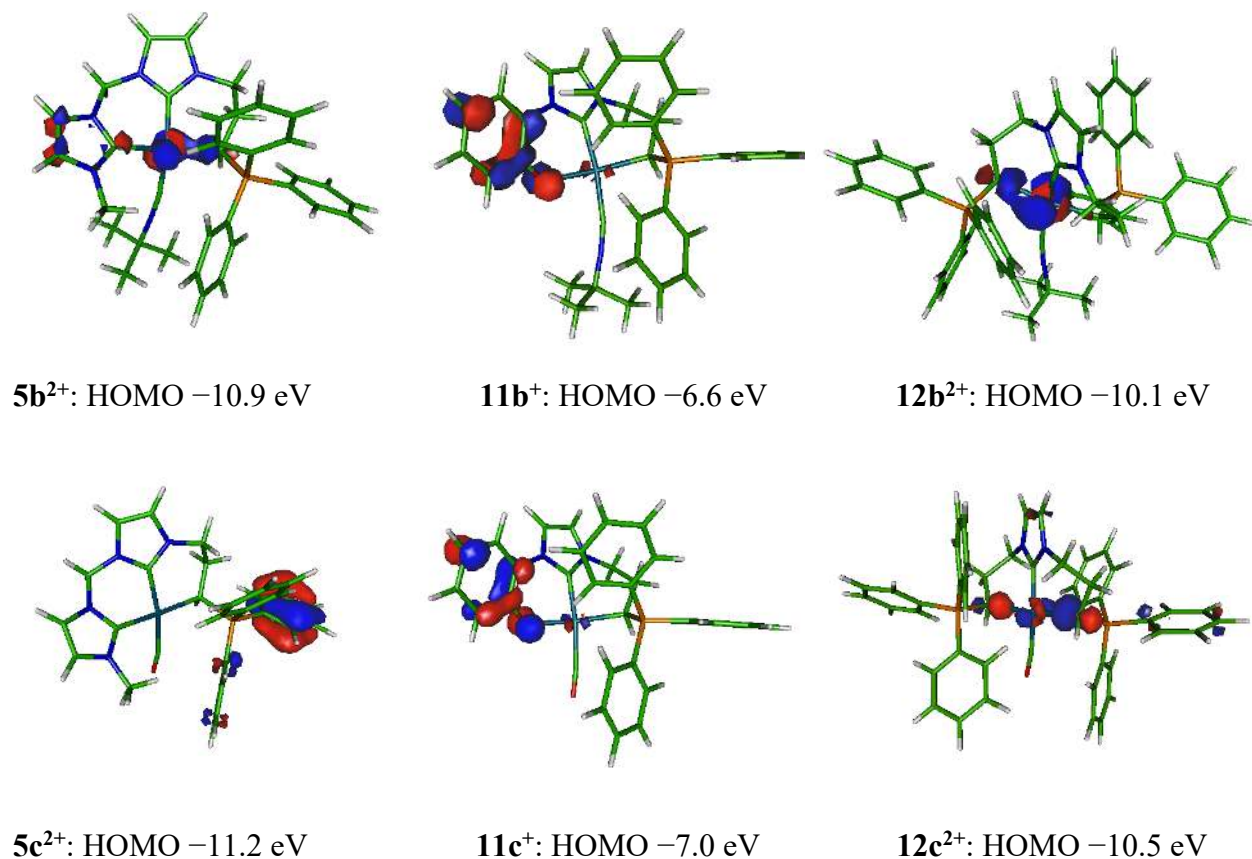


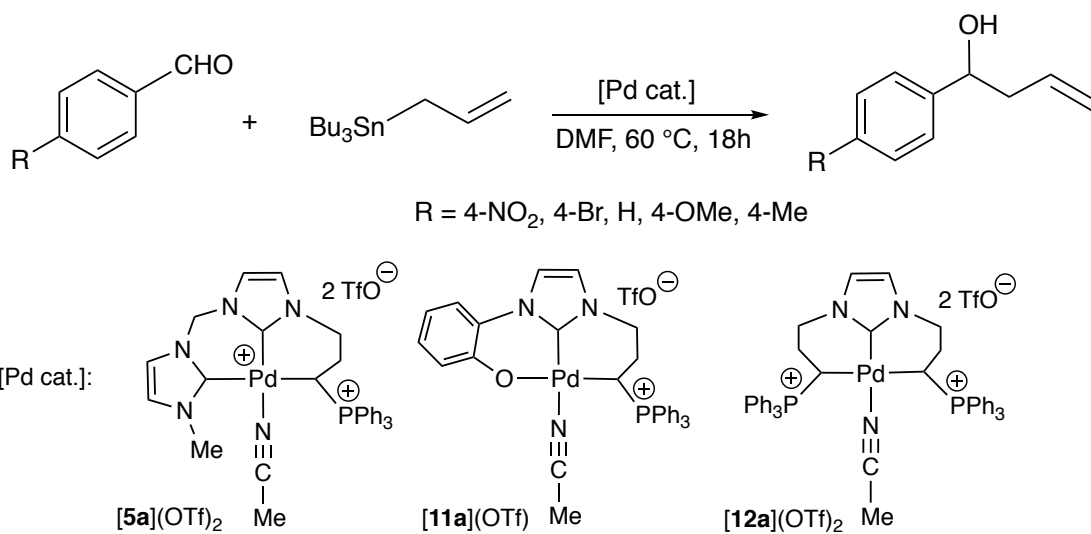
Figure 3. Representation of HOMOs of Pd complexes **5²⁺** (*left*), **11⁺** (*middle*) and **12²⁺** (*right*) with corresponding energy values (**b**: L = CN*t*Bu, *up*; **c**: L = CO, *down*). For complex **12²⁺**, only the HOMOs of the *dl*-isomer are represented. PBE-D3/6-31G**/LANL2DZ*(Pd) level of calculation.

Considering that the oxidation potential (E_p^{ox}) of a complex reflects generally the electronic properties of its ligand, the ylide-based Pd–NCCH₃ complexes [**5a**](OTf)₂, [**11a**](OTf) and [**12a**](OTf)₂ and their corresponding *ortho*-metallated forms were investigated by cyclic voltammetry (Table 1). All oxidations were found to be irreversible with the E_p^{ox} values varying according to the donating character of the pincer ligand: the electron-rich bis(ylide) Pd complex [**12a**](OTf)₂ being indeed the most easily oxidized. Electrochemical measurements indicated also that going from the pincer complexes to their *ortho*-metallated forms results in a significant decrease of the E_p^{ox} values as expected since the latter complexes were formed by deprotonation of the former. The same relative variation observed for the E_p^{ox} values and the IR ν_{CO} and ν_{CN} stretching frequencies corroborate the assumption that the redox events are probably based on the Pd center.

2.4 Catalytic investigations

To evaluate the role of the structure of the pincer ligand on catalytic properties, the Pd-catalyzed allylation of aldehydes with allyltributyltin was selected. It was indeed reported that this transformation is efficiently catalyzed by pincer Pd(II) complexes bearing strongly σ -donating ligands,³² which contribute to increase the electron density at the metal and therefore the nucleophilic character of the allyl fragment in a η^1 -allyl-coordinated pincer complex identified as active catalytic intermediate.³³ The reactions were performed with various *p*-substituted aldehydes characterizing by different electronic requirement in the presence of catalytic amounts of the phosphonium ylide-based pincer Pd(II) complexes **[5a]**(OTf)₂, **[11a]**(OTf) and **[12a]**(OTf)₂ in DMF at 60 °C for 18 hours (Table 2). Whatever the aldehyde, the bis(ylide) Pd complex **[12a]**(OTf)₂ complex showed the highest catalytic activity, the bis(NHC) complex **[5a]**(OTf)₂ being the least active. For example, benzaldehyde is converted in 81% after 18 h at 60 °C when **[12a]**(OTf)₂ is used as catalyst (5.0 mol %, entry 16), while in the same conditions, complexes **[5a]**(OTf)₂ and **[11a]**(OTf) produce the desired product in 30 and 58%, respectively (entries 14-15). With complex **[12a]**(OTf)₂, the catalytic charge could be lowered to 1.0 mol % while keeping an acceptable yield (ca. 60%, entry 17). Homo-allylic alcohol products were obtained in higher yields with activated aldehydes, such as *p*-NO₂ and *p*-Br benzaldehydes. Gratifyingly, *p*-NO₂ benzaldehyde could be properly converted in the presence of 0.5 mol % of **[12a]**(OTf)₂ (80%, entry 6), being able to decrease the catalytic charge to 0.1 mol % (46%, entry 7). As expected, the electronically deactivated *p*-Me and *p*-MeO benzaldehydes were found to be less reactive, the bis(ylide) Pd complex **[12a]**(OTf)₂ allowing the formation of corresponding coupling products in 62 and 56% yield using a 5 mol % catalytic charge (entries 21 and 24).³⁴ The catalytic activity of complex **[12a]**(OTf)₂ is comparable to that reported with anionic [PCP] Pd(II) complexes,³²⁻³³ but it appears to be higher than that observed with NHC Pd(II) complexes.³⁵

Table 2. Catalytic allylation of aldehydes with phosphonium ylide-based pincer Pd complexes **[5a](OTf)₂**, **[11a](OTf)**, and **[12a](OTf)₂**.^a



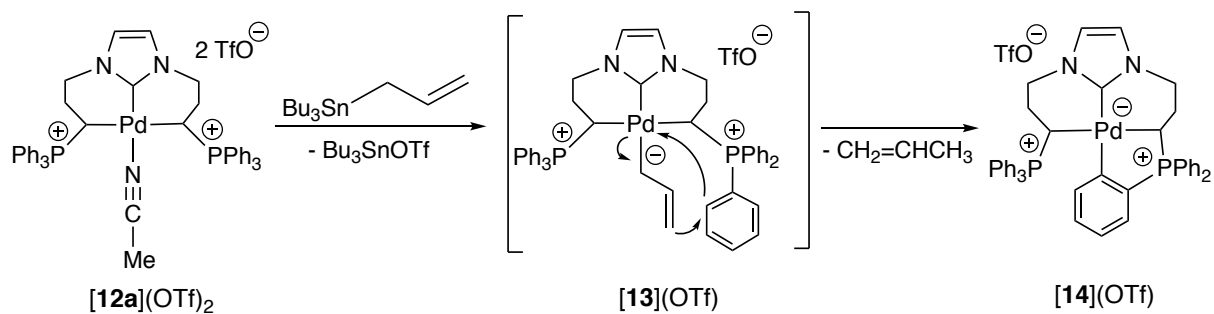
Entry	R	Complex	Cat. [%]	Conv. ^b
1	NO ₂	[5a](OTf)₂	5	50 (40)
2	NO ₂	[11a](OTf)	5	> 98 (92)
3	NO ₂	[11a](OTf)	1	78 (74)
4	NO ₂	[12a](OTf)₂	5	> 98 (97)
5	NO ₂	[12a](OTf)₂	1	86 (78)
6	NO ₂	[12a](OTf)₂	0.5	80 (70)
7	NO ₂	[12a](OTf)₂	0.1	46 (40)
8	NO ₂	-	-	11
9	Br	[5a](OTf)₂	5	35
10	Br	[11a](OTf)	5	66 (57)
11	Br	[12a](OTf)₂	5	91 (85)
12	Br	[12a](OTf)₂	1	34
13	Br	-	-	0
14	H	[5a](OTf)₂	5	30
15	H	[11a](OTf)	5	58 (42)
16	H	[12a](OTf)₂	5	81 (75)
17	H	[12a](OTf)₂	1	60 (54)
18	H	-	-	0
19	Me	[5a](OTf)₂	5	20

20	Me	[11a](OTf)	5	57 (45)
21	Me	[12a](OTf) ₂	5	62 (55)
22	MeO	[5a](OTf) ₂	5	10
23	MeO	[11a](OTf)	5	19
24	MeO	[12a](OTf) ₂	5	56 (45)

^a All reactions were performed with 1.0 equiv. of aldehyde and 1.2 equiv. of allyltributyltin in DMF at 60 °C for 18 h. ^b Conversion determined by ¹H NMR, isolated yields in parenthesis.

These results indicate that the ligand structure of pincer Pd complexes influence significantly the catalytic properties. The superiority of complex [**12a**](OTf)₂ can be attributed to the stronger donating properties of the *C,C,C*-NHC, bis(ylide) pincer ligand which would favor the nucleophilic attack of the η^1 -allyl-pincer intermediate on the aldehyde. These findings are therefore in agreement with experimental and calculated IR ν_{CO} and ν_{CN} frequencies. With a similar donor character, the difference in activity observed between complexes [**5a**](OTf)₂ and [**11a**](OTf) also suggest that other factors may play a role and that a good balance in the catalytic system is generally required in order to benefit at all elementary steps.

To gain more insight on the catalytic mechanism, stoichiometric reactions were carried out from bis(ylide) complex [**12a**](OTf)₂. The stability of [**12a**](OTf)₂ in DMF at 60 °C for 18 h was first confirmed by ³¹P NMR monitoring. In the presence of a stoichiometric quantity of benzaldehyde in DMF at 60 °C for 18 h, the complex [**12a**](OTf)₂ was found to be unreactive. On the other hand, the addition on [**12a**](OTf)₂ of a stoichiometric amount of allyltributyltin in the same conditions led cleanly to the formation of the *ortho*-metallated complex [**14**](OTf) (Scheme 9).³⁶ This result is in favor of the formation of the η^1 -allyl-Pd pincer complex [**13**](OTf), which in the absence of an electrophile, would stabilize by formation of the *ortho*-metallated product [**14**](OTf), the electron-rich allyl moiety playing here the role of an internal base. This reactivity is confirmed by the complete conversion of [**12a**](OTf)₂ into its *ortho*-metallated form [**14**](OTf) upon addition of KHMDS base in THF. In accordance with its high stability and the role of the η^1 -allyl ligand in the Pd intermediate [**13**](OTf), the pre-catalyst [**12a**](OTf)₂ was recovered after catalysis by extraction with CH₂Cl₂ in mixture with its *ortho*-metallated form [**14**](OTf).



Scheme 9. Proposed mechanism of formation of the *ortho*-metallated complex **[14](OTf)** from **[12a](OTf)₂** in the presence of allyltributyltin.

To further investigate the role of the strongly donating bis(ylide) pincer ligand in the η^1 -allyl-Pd catalytic intermediate **13⁺**, DFT studies were undertaken at the PBE-D3/6-31G**/LANL2DZ*(Pd) level of calculation (Figure 4).³¹ The difference in energy found between the OMs of **13⁺** and those of the pre-catalyst **12a²⁺** is consistent with the different overall charge [**13⁺** (+1) and **12a²⁺** (+2)], the MO levels of **13⁺** being indeed shifted up to higher energy compared to **12a²⁺** as illustrated with the relative HOMO energies (**12a²⁺**: -10.1 eV; **13⁺**: -6.0 eV). A close inspection indicates also a significant change in the nature of the HOMOs, namely that the HOMO initially localized on the two Csp^3 -Pd bonds in **12a²⁺** is now strongly located on the π -system of the coordinated η^1 -allyl fragment in **13⁺**, suggesting a preferential interaction of the allyl moiety with electrophiles.

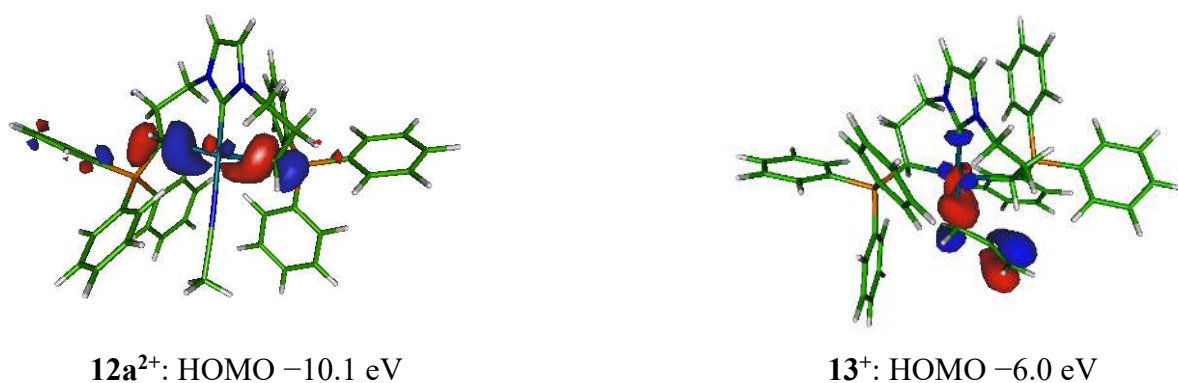
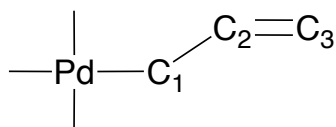


Figure 4. Representation of the HOMOs of pre-catalyst **12a²⁺** and η^1 -allyl-Pd pincer intermediate **13⁺** with corresponding energy values. In both cases, only the HOMOs of the *dl*-isomers are represented. PBE-D3/6-31G**/LANL2DZ*(Pd) level of calculation.

Based on these findings, the chemical reactivity of $\mathbf{13}^+$ was further investigated using Fukui functions f condensed on Quantum Theory of Atoms in Molecules (QTAIM) or on Electron Localization Function (ELF) basins (Table 3). The largest f_{ELF} value (0.22) is obtained for the ELF valence basin of the allyl termini V(C2,C3), suggesting that it is the most sensitive bond to electrophilic attack. It is supported by f_{QTAIM} taking its maximum value for the C3 carbon atom ($f_{\text{QTAIM}}(\text{C3}) = 0.29$), in agreement with the reactivity observed experimentally and with previous calculations performed on related models.^{33b}

Table 3. Selected values of atomic QTAIM charges and Fukui functions f condensed on QTAIM and ELF basins for the η^1 -allyl ligand in Pd complex $\mathbf{13}^+$. PBE-D3/6-31G**/LANL2DZ*(Pd) level of calculation.



	Pd	C1	C2	C3
Atomic charges (QTAIM)	-0.4	-0.3	-0.1	-0.2
f_{QTAIM}	0.16	0.25	0.08	0.29
f_{ELF}	C(Pd): 0.13	V(Pd, C1): 0.17	-	V(C2,C3): 0.22

3. CONCLUSION

An isostructural family of NHC core, phosphonium ylide-based Pd(II) pincer complexes where the third extremity can be modified was described according to two distinct synthetic pathways. While the difference in acidity between the cationic imidazolium and phosphonium moieties led to the development of a two-step method, the most direct route to the phosphonium ylide-based Pd(II) pincers involves the passage through the formation of *ortho*-metallated Pd complexes. Thanks to their high stability and availability, these *ortho*-metallated species serve as reservoirs for more reactive pincer complexes as illustrated with the formation of Pd–NCCH₃ adducts upon acidic treatment. Based on IR ν_{CO} and ν_{CN} frequencies, E_{p}^{ox} values and on the determination of MOs, a direct comparison between NHC (A), phenolate (B) and phosphonium ylide (C) moieties in related complexes [NHC(A_aB_bC_c)PdL][OTf] ($a + b + c = 2$; L = NCCH₃, CN*t*Bu or CO) was undertaken, evidencing the stronger donor character of phosphonium ylides. This difference in donor

ability is valued for the first time in homogeneous catalysis for the Pd-catalyzed allylation of aldehydes. In this process, the intermediate formation of a η^1 -allyl-Pd pincer complex was confirmed on the basis of experimental and theoretical studies. Other catalytic transformations are now targeted with these extremely electron-rich carbon-based pincer ligands. Future studies will also aim to extend this methodology to the preparation of pincer complexes featuring phosphonium ylide extremities with different P-substituents and/or other donor moieties such as amines and phosphines.

EXPERIMENTAL SECTION

General Remarks. All manipulations were performed under an inert atmosphere of dry nitrogen by using standard vacuum line and Schlenk tube techniques. Glassware was dried at 120 °C in an oven for at least three hours. Dry and oxygen-free organic solvents (THF, Et₂O, CH₂Cl₂, toluene, pentane) were obtained using a LabSolv (Innovative Technology) solvent purification system. Acetonitrile was dried and distilled over P₂O₅ under argon. All other reagent-grade chemicals were purchased from commercial sources and used as received. Chromatographic purification was carried out on silica gel (SiO₂, 63–200 μ m). ¹H, ³¹P, and ¹³C NMR spectra were obtained on Bruker AV300, AV400 or NEO600 spectrometers. NMR chemical shifts δ are in ppm, with positive values to high frequency relative to the tetramethylsilane reference for ¹H and ¹³C and to 85% H₃PO₄ for ³¹P. If necessary, additional information on the carbon signal attribution was obtained using ¹³C{¹H, ³¹P}, *J*-modulated spin-echo (JMOD) ¹³C{¹H}, ¹H–¹³C HMQC, and/or HMBC experiments. MS spectra (ESI mode) were performed by the mass spectrometry service of the “Institut de Chimie de Toulouse”. Elemental analyses were carried out by the elemental analysis service of the “LCC” using a Perkin Elmer 2400 series II analyzer. Voltammetric measurements were performed by the electrochemistry service of the “LCC”. 3-((1H-imidazol-1-yl)-methyl)-1-methyl-1H-imidazol-3-ium iodide [**1**]^I²⁰ and 1-(2-hydroxyphenyl)imidazole **6**²⁶ were prepared according to previously described procedures.

NB: All compounds were found to be highly hygroscopic and difficult to weigh in air.

Synthesis of pre-ligand [**2**](OTf)₃

A solution of 3-((1H-imidazol-1-yl)-methyl)-1-methyl-1H-imidazol-3-ium iodide [**1**]^I (1.04 g, 3.58 mmol) and 3-bromopropyl triphenylphosphonium bromide (1.84 g, 3.96 mmol) in DMF (70 mL) under nitrogen was stirred at 120 °C for 12 hours. After evaporation of the solvent under vacuum, the remaining solid was heated at 70 °C for 2 hours. The solid residue was dissolved in a minimum of CH₃CN (10 mL), and after few minutes a solid precipitate

appeared. After filtration, the solid residue (2.45 g, 3.26 mmol) and sodium triflate (1.68 g, 9.78 mmol) were stirred in CH₃CN (30 mL) at room temperature for 12 hours. The mixture was filtered through Celite, and the resulting solution was evaporated to dryness under reduced pressure. The crude product was dissolved in CH₂Cl₂ (20 mL), and washed with water (20 mL). The aqueous phase was then extracted with CH₂Cl₂ (3 x 20 mL). The combined organic phases were dried over MgSO₄ and after evaporation of the solvent under vacuum, [2](OTf)₃ was obtained as a white powder (2.98 g, 91%). ³¹P{¹H} NMR (162 MHz, CD₃CN, 25 °C): δ = 25.0 (s); ¹H NMR (400 MHz, CD₃CN, 25 °C) δ = 9.31 (s, 1H, N₂CH), 9.10 (s, 1H, N₂CH), 7.86–7.91 (m, 3H, H_{Ar}), 7.70–7.77 (m, 14H, H_{Ar}), 7.51 (t, J_{HH} = 1.8 Hz, 1H, H_{Ar}), 7.44 (t, J_{HH} = 1.8 Hz, 1H, H_{Ar}), 6.54 (s, 2H, NCH₂N), 4.40 (t, J_{HH} = 7.1 Hz, 2H, NCH₂), 3.88 (s, 3H, NCH₃), 3.30–3.37 (m, 2H, PCH₂), 2.13–2.25 (m, 2H, CH₂); ¹³C{¹H} NMR (101 MHz, CD₃CN, 25 °C): δ = 138.8 (s, N₂CH), 138.6 (s, N₂CH), 136.3 (d, J_{CP} = 3.0 Hz, CH_{Ph}), 134.8 (d, J_{CP} = 10.1 Hz, CH_{Ph}), 131.3 (d, J_{CP} = 12.1 Hz, CH_{Ph}), 125.7 (s, CH_{Im}), 124.4 (s, CH_{Im}), 123.6 (s, CH_{Im}), 123.3 (s, CH_{Im}), 121.5 (q, J_{CF} = 320.9 Hz, CF₃), 118.6 (d, J_{CP} = 86.5 Hz, C_{Ph}), 59.5 (s, NCH₂N), 50.4 (d, J_{CP} = 21.1 Hz, NCH₂), 37.5 (s, NCH₃), 23.6 (d, J_{CP} = 2.0 Hz, CH₂), 20.1 (d, J_{CP} = 55.3 Hz, PCH₂); MS (ES⁺): m/z: 765.1 [M – CF₃SO₃]⁺; elemental analysis for C₃₂H₃₂F₉N₄O₉PS₃: calcd, C 42.02, H 3.53, N 6.12; found, C 41.87, H 3.36, N 6.01.

Synthesis of complex [3](OTf)

[2](OTf)₃ (0.16 g, 0.17 mmol) and bis(acetonitrile)-palladium chloride (0.06 g, 0.22 mmol) were dissolved in dry CH₃CN (12 mL). Triethylamine (60 μL, 0.43 mmol) was then added and the suspension was heated at 60 °C for 4 hours. After filtration over Celite, the solvent was removed under vacuum. The solid residue was dissolved in CH₂Cl₂ (20 mL), the solution was washed several times with water and dried over MgSO₄. After evaporation of the solvent, [3](OTf) was obtained as a yellow solid (0.10 g, 75%). Additional purification may be performed if necessary by passing the complex [3](OTf) over a small column of alumina (eluent CH₂Cl₂/EtOAc/CH₃OH). ³¹P{¹H} NMR (121 MHz, CD₃CN, 25 °C): δ = 23.6 (s); ¹H NMR (300 MHz, CD₃CN, 25 °C) δ = 7.83–7.89 (m, 3H, H_{Ar}), 7.70–7.79 (m, 12H, H_{Ar}), 7.34 (t, J_{HH} = 2.2 Hz, 2H, H_{Ar}), 7.04 (d, J_{HH} = 2.0 Hz, 1H, H_{Ar}), 6.97 (d, J_{HH} = 2.0 Hz, 1H, H_{Ar}), 6.23 (d, J_{HH} = 13.1 Hz, 1H, NCH₂N), 6.07 (d, J_{HH} = 13.1 Hz, 1H, NCH₂N), 4.77–4.87 (m, 1H, NCH₂), 4.51–4.61 (m, 1H, NCH₂), 3.80 (s, 3H, NCH₃), 3.21–3.56 (m, 2H, PCH₂), 2.14–2.35 (m, 2H, CH₂); ¹³C{¹H} NMR (75 MHz, CD₃CN, 25 °C): δ = 159.0 (s, N₂C), 158.5 (s, N₂C), 136.1 (d, J_{CP} = 3.0 Hz, CH_{Ph}), 134.7 (d, J_{CP} = 10.6 Hz, CH_{Ph}), 131.3 (d, J_{CP} = 12.8 Hz, CH_{Ph}), 123.8 (s, CH_{Im}), 122.6 (s, CH_{Im}), 122.5 (s, CH_{Im}), 122.2 (s, CH_{Im}), 121.6 (q, J_{CF} = 320.8 Hz,

CF₃), 119.0 (d, J_{CP} = 86.8 Hz, C_{Ph}), 63.5 (s, NCH₂N), 50.8 (d, J_{CP} = 21.1 Hz, NCH₂), 38.8 (s, NCH₃), 25.2 (d, J_{CP} = 3.0 Hz, CH₂), 20.3 (d, J_{CP} = 54.4 Hz, PCH₂); MS (ES⁺): m/z : 642.9 [M – CF₃SO₃]⁺; elemental analysis for C₃₀H₃₀Cl₂F₃N₄O₃PPdS: calcd, C 45.50, H 3.82, N 7.07; found, C 45.81, H 3.81, N 6.74.

Synthesis of complex [4](OTf)

1st method: Complex [3](OTf) (0.04 g, 0.051 mmol) and anhydrous Cs₂CO₃ (0.05 g, 0.15 mmol) were dissolved in CH₃CN (4 mL), and the suspension was stirred at 60 °C for 16 hours. After filtration over Celite, the solvent was evaporated under vacuum, affording complex [4](OTf) as a white solid (0.035 g, 94%). Recrystallization from CH₂Cl₂/pentane at –20 °C gave pale yellow crystals suitable for X-ray diffraction.

2nd method: A mixture of [2](OTf)₃ (0.10 g, 0.11 mmol), PdCl₂ (0.02 g, 0.11 mmol), and anhydrous Cs₂CO₃ (0.18 g, 0.55 mmol) was stirred at 60 °C in CH₃CN (10 mL) for 12 hours. After filtration over Celite and evaporation of the solvent under vacuum, the crude residue was dissolved in CH₂Cl₂ (10 mL), and the solution was filtered over Celite. After evaporation of the solvent, the resulting solid was washed with Et₂O (3 x 10 mL) affording [4](OTf) as a pale yellow powder (0.05 g, 69%).

³¹P{¹H} NMR (162 MHz, CD₃CN, 25 °C): δ = 30.4 (s); ¹H NMR (400 MHz, CD₃CN, 25 °C) δ = 7.76–7.83 (m, 6H, H_{Ar}), 7.67–7.70 (m, 2H, H_{Ar}), 7.60–7.65 (m, 1H, H_{Ar}), 7.48–7.51 (m, 2H, H_{Ar}), 7.38 (d, J_{HH} = 1.9 Hz, 1H, H_{Ar}), 7.21–7.25 (m, 1H, H_{Ar}), 7.21 (d, J_{HH} = 1.9 Hz, 1H, H_{Ar}), 7.13 (d, J_{HH} = 1.9 Hz, 1H, H_{Ar}), 7.06–7.14 (m, 2H, H_{Ar}), 6.98 (d, J_{HH} = 1.9 Hz, 1H, H_{Ar}), 6.07 (d, J_{HH} = 13.0 Hz, 1H, NCH₂N), 6.01 (d, J_{HH} = 13.0 Hz, 1H, NCH₂N), 3.93 (td, J_{HH} = 3.7, 13.3 Hz, 1H, NCH₂), 3.72 (s, 3H, NCH₃), 3.02 (brt, J_{HH} = 11.7 Hz, 1H, NCH₂), 2.64 (dd, J_{HH} = 2.6, 9.2 Hz, 1H, PCH), 2.41–2.46 (m, 1H, CH₂), 2.05–2.26 (m, 1H, CH₂); ¹³C{¹H} NMR (101 MHz, CD₃CN, 25 °C): δ = 179.9 (d, J_{CP} = 34.2 Hz, C_{Ph}), 178.8 (d, J_{CP} = 6.0 Hz, N₂C), 177.7 (d, J_{CP} = 7.0 Hz, N₂C), 142.6 (d, J_{CP} = 19.1 Hz, CH_{Ph}), 139.2 (d, J_{CP} = 115.7 Hz, C_{Ph}), 134.4 (d, J_{CP} = 9.0 Hz, CH_{Ph}), 134.03 (d, J_{CP} = 2.0 Hz, CH_{Ph}), 134.0 (d, J_{CP} = 9.0 Hz, CH_{Ph}), 133.7 (d, J_{CP} = 3.0 Hz, CH_{Ph}), 131.3 (d, J_{CP} = 20.1 Hz, CH_{Ph}), 130.6 (d, J_{CP} = 10.1 Hz, CH_{Ph}), 130.3 (d, J_{CP} = 3.0 Hz, CH_{Ph}), 130.0 (d, J_{CP} = 12.1 Hz, CH_{Ph}), 129.3 (d, J_{CP} = 87.5 Hz, C_{Ph}), 127.5 (d, J_{CP} = 55.3 Hz, C_{Ph}), 125.4 (d, J_{CP} = 7.0 Hz, CH_{Ph}), 122.9 (s, CH_{Im}), 122.7 (s, CH_{Im}), 121.6 (q, J_{CF} = 320.8 Hz, CF₃), 121.5 (s, CH_{Im}), 120.4 (s, CH_{Im}), 63.8 (s, NCH₂N), 52.5 (d, J_{CP} = 3.0 Hz, NCH₂), 39.5 (s, NCH₃), 25.7 (d, J_{CP} = 3.0 Hz, CH₂), 17.3 (d, J_{CP} = 36.2 Hz, PCH); MS (ES⁺): m/z : 569.1 [M – CF₃SO₃]⁺; HRMS (ES⁺): calcd for C₂₉H₂₈N₄PPd, 569.1097; found, 569.1100; elemental analysis for C₃₀H₂₈F₃N₄O₃PPdS.0.5 H₂O: calcd, C 49.49, H 4.01, N 7.70; found, C 49.43, H 3.91, N 7.22.

Synthesis of complex [5a](OTf)₂

TfOH (0.5 M in CH₃CN, 0.14 mL, 0.067 mmol) was added at -40 °C to a solution of complex [4](OTf) (0.05 g, 0.069 mmol) in CH₃CN (5 mL). The mixture was warmed to room temperature for 2 hours. After filtration over Celite, the solvent was removed under vacuum, and complex [5a](OTf)₂ was obtained as a pale yellow powder (0.06 g, 91%). ³¹P{¹H} NMR (202 MHz, CD₃CN, 25 °C): δ = 33.9 (s); ¹H NMR (500 MHz, CD₃CN, 25 °C) δ = 7.71–7.77 (m, 9H, H_{Ar}), 7.57–7.61 (m, 6H, H_{Ar}), 7.33 (d, *J*_{HH} = 1.8 Hz, 1H, H_{Ar}), 7.18 (d, *J*_{HH} = 1.8 Hz, 1H, H_{Ar}), 7.08 (d, *J*_{HH} = 1.8 Hz, 1H, H_{Ar}), 6.97 (d, *J*_{HH} = 1.8 Hz, 1H, H_{Ar}), 5.97 (d, *J*_{HH} = 13.2 Hz, 1H, NCH₂N), 5.65 (d, *J*_{HH} = 13.2 Hz, 1H, NCH₂N), 4.13–4.15 (m, 1H, NCH₂), 3.82–3.87 (m, 1H, NCH₂), 3.72 (s, 3H, NCH₃), 3.44–3.49 (m, 1H, CH₂), 2.45–2.57 (m, 1H, PCH), 1.90–1.95 (m, 1H, CH₂); ¹³C{¹H} NMR (125.8 MHz, CD₃CN, 25 °C): δ = 168.6 (s, N₂C), 158.1 (s, N₂C), 134.8 (d, *J*_{CP} = 8.8 Hz, CH_{Ph}), 134.6 (d, *J*_{CP} = 2.5 Hz, CH_{Ph}), 130.5 (d, *J*_{CP} = 11.3 Hz, CH_{Ph}), 124.4 (d, *J*_{CP} = 83.0 Hz, C_{Ph}), 124.0 (s, CH_{Im}), 122.6 (s, CH_{Im}), 122.5 (s, CH_{Im}), 122.2 (s, CH_{Im}), 121.8 (q, *J*_{CF} = 320.9 Hz, CF₃), 63.1 (s, NCH₂N), 52.6 (d, *J*_{CP} = 12.6 Hz, NCH₂), 38.7 (s, NCH₃), 25.6 (s, CH₂), 9.9 (d, *J*_{CP} = 32.7 Hz, PCH); MS (ES⁺): *m/z*: 719.1 [M – CH₃CN – CF₃SO₃]⁺; HRMS (ES⁺): calcd for C₃₀H₂₉F₃N₄O₃PPdS, 719.0696; found, 719.0709; elemental analysis for C₃₃H₃₂F₆N₅O₆PPdS₂·H₂O: calcd, C 42.70, H 3.69, N 7.55; found, C 42.16, H 3.24, N 8.21.

Synthesis of complex [5b](OTf)₂

t-butyl isocyanide (9.32 μL, 0.082 mmol) was added at -78 °C to a solution of complex [5a](OTf)₂ (0.05 g, 0.055 mmol) in CH₂Cl₂ (3 mL). The mixture was warmed to room temperature for 4 hours. After filtration over Celite, the solvent was removed under vacuum, and complex [5b](OTf)₂ was obtained as a pale yellow powder (0.049 g, 94%). ³¹P{¹H} NMR (162 MHz, CD₂Cl₂, 25 °C): δ = 35.0 (s); ¹H NMR (500 MHz, CD₂Cl₂, 25 °C) δ = 7.78–7.70 (m, 9H, H_{Ar}), 7.66–7.61 (m, 6H, H_{Ar}), 7.59 (d, *J*_{HH} = 1.8 Hz, 1H, H_{Ar}), 7.46 (d, *J*_{HH} = 1.8 Hz, 1H, H_{Ar}), 7.09 (d, *J*_{HH} = 1.8 Hz, 1H, H_{Ar}), 6.99 (d, *J*_{HH} = 1.8 Hz, 1H, H_{Ar}), 6.41 (d, *J*_{HH} = 13.2 Hz, 1H, NCH₂N), 5.80 (d, *J*_{HH} = 13.2 Hz, 1H, NCH₂N), 4.27–4.19 (m, 1H, NCH₂), 4.07–4.01 (m, 1H, NCH₂), 3.84 (s, 3H, NCH₃), 3.44–3.34 (m, 1H, PCH), 2.53–2.35 (m, 2H, CH₂), 1.06 (s, 9H, *t*Bu); ¹³C{¹H} NMR (101 MHz, CD₃CN, 25 °C)*: δ = 167.5 (s, N₂C), 163.1 (s, N₂C), 134.6 (d, *J*_{CP} = 2.5 Hz, CH_{Ph}), 134.4 (d, *J*_{CP} = 8.8 Hz, CH_{Ph}), 130.4 (d, *J*_{CP} = 11.3 Hz, CH_{Ph}), 124.0 (d, *J*_{CP} = 83.0 Hz, C_{Ph}), 123.4 (s, CH_{Im}), 123.2 (s, CH_{Im}), 122.6 (s, CH_{Im}), 121.7 (s, CH_{Im}), 121.4 (q, *J*_{CF} = 320.9 Hz, CF₃), 62.9 (s, NCH₂N), 59.7 (s, C(CH₃)₃), 51.5 (d, *J*_{CP} = 12.6 Hz, NCH₂), 39.2 (s, NCH₃), 29.5 (s, CH₃), 25.5 (s, CH₂), 6.5 (d, *J*_{CP} = 32.7 Hz, PCH); MS (ES⁺): *m/z*: 719.1 [M – *t*BuNC – CF₃SO₃]⁺; HRMS (ES⁺): calcd for C₃₀H₂₉F₃N₄O₃PPdS,

719.0696; found, 719.0711; elemental analysis for C₃₆H₃₈F₆N₅O₆PPdS₂. H₂O: calcd, C 44.57, H 4.16, N 7.22; found, C 44.16, H 3.98, N 8.41. * The ¹³C NMR resonance of the CN quaternary carbon atom of coordinated *t*-BuNC was not observed.

Synthesis of pre-ligand [7]Br₂

1-(2-hydroxyphenyl)imidazole **6** (0.50 g, 3.12 mmol) and (3-bromo-propyl)-triphenylphosphonium bromide (0.96 g, 2.08 mmol) were heated at 120 °C in C₆H₅Cl (30 mL) for 15 hours. After evaporation of the solvent, the crude residue was washed with Et₂O (3 x 80 mL) affording a white powder (1.19 g, 92%). Recrystallization from CH₃CN at room temperature gave [7]Br₂ as colorless crystals suitable for X-ray diffraction. ³¹P{¹H} NMR (162 MHz, CDCl₃, 25 °C): δ = 24.3 (s); ¹H NMR (400 MHz, CDCl₃, 25 °C): δ = 9.91 (s, 1H, N₂CH), 8.29 (s, 1H, H_{Ar}), 7.85–7.80 (m, 6H, H_{Ar}), 7.77–7.72 (m, 3H, H_{Ar}), 7.67–7.63 (m, 7H, H_{Ar}), 7.53 (d, *J*_{HH} = 8.2 Hz, 1H, H_{Ar}), 7.37 (d, *J*_{HH} = 7.9 Hz, 1H, H_{Ar}), 7.31 (s, 1H, H_{Ar}), 7.16 (t, *J*_{HH} = 7.4 Hz, 1H, H_{Ar}), 6.83 (d, *J*_{HH} = 7.7 Hz, 1H, H_{Ar}), 5.08 (m, 2H, NCH₂), 3.93 (m, 2H, PCH₂), 2.46 (m, 2H, CH₂). ¹³C{¹H} NMR (101 MHz, CDCl₃, 25 °C): δ = 150.3 (s, C_{Ph}), 136.2 (s, N₂CH), 135.3 (d, *J*_{CP} = 3.0 Hz, CH_{Ph}), 134.0 (d, *J*_{CP} = 10.6 Hz, CH_{Ph}), 131.3 (s, CH_{Ph}), 130.7 (d, *J*_{CP} = 12.8 Hz, CH_{Ph}), 125.0 (s, CH_{Ph}), 123.2 (s, CH_{Ph}), 123.0 (s, CH_{Ph}), 122.2 (s, C_{Ph}), 120.6 (s, CH_{Im}), 118.9 (s, CH_{Im}), 117.6 (d, *J*_{CP} = 86.8 Hz, C_{Ph}), 49.0 (d, *J*_{CP} = 21.1 Hz, NCH₂), 24.9 (d, *J*_{CP} = 3.0 Hz, CH₂), 20.2 (d, *J*_{CP} = 54.4 Hz, PCH₂); MS (ES⁺): *m/z*: 543.1 [M – Br]⁺; HRMS (ES⁺): calcd for C₃₀H₂₉N₂OPPdBr, 543.1201; found, 543.1205; elemental analysis for C₃₀H₂₉Br₂N₂OP.H₂O: calcd, C 56.09, H 4.86, N 4.36; found, C 56.0, H 4.66, N 4.72.

Synthesis of pre-ligand [7](OTf)₂

[7]Br₂ (0.97 g, 1.56 mmol) and sodium trifluoromethanesulfonate (0.67 g, 3.90 mmol) were dissolved in CH₂Cl₂ (60 mL) and the solution was stirred at room temperature for 12 hours. After evaporation of the solvent, the crude residue was washed with water (30 mL). The organic layer was extracted with CH₂Cl₂ (2 x 30 mL) and dried over Na₂SO₄. After evaporation of the solvent, [7](OTf)₂ was obtained as a white powder (1.19 g, 95%). ³¹P{¹H} NMR (162 MHz, CDCl₃, 25 °C): δ = 23.9 (s); ¹H NMR (400 MHz, CDCl₃, 25 °C): δ = 9.20 (s, 1H, N₂CH), 7.78–7.68 (m, 17H, H_{Ar}), 7.41 (brs, 1H, H_{Ar}), 7.27 (m, 1H, H_{Ar}), 7.21–7.15 (m, 2H, H_{Ar}), 6.83 (t, *J*_{HH} = 7.7 Hz, 1H, H_{Ar}), 4.66 (m, 2H, NCH₂), 3.50 (m, 2H, PCH₂), 2.30 (m, 2H, CH₂). ¹³C{¹H} NMR (101 MHz, CDCl₃, 25 °C): δ = 151.2 (s, C_{Ph}), 136.0 (s, N₂CH), 135.4 (d, *J*_{CP} = 3.0 Hz, CH_{Ph}), 133.7 (d, *J*_{CP} = 10.6 Hz, CH_{Ph}), 131.6 (s, CH_{Ph}), 130.7 (d, *J*_{CP} = 12.8 Hz, CH_{Ph}), 124.6 (s, CH_{Ph}), 123.5 (s, CH_{Ph}), 122.5 (s, CH_{Ph}), 122.3 (s, C_{Ph}), 120.6 (q, *J*_{CP}

= 319.9 Hz, CF₃), 119.9 (s, CH_{Im}), 118.7 (s, CH_{Im}), 117.4 (d, J_{CP} = 86.8 Hz, C_{Ph}), 49.1 (d, J_{CP} = 21.1 Hz, NCH₂), 24.4 (d, J_{CP} = 3.0 Hz, CH₂), 19.6 (d, J_{CP} = 54.4 Hz, PCH₂); MS (ES⁺): m/z : 613.2 [M - CF₃SO₃]⁺; elemental analysis for C₃₀H₂₉F₆N₂O₇PS₂: calcd, C 50.40, H 3.83, N 3.67; found, C 51.08, H 3.72, N 3.94.

Synthesis of complex [8](OTf)

A mixture of [7](OTf)₂ (0.20 g, 0.26 mmol), PdCl₂ (0.05 g, 0.26 mmol), anhydrous K₂CO₃ (0.11 g, 0.78 mmol), and pyridine (63.3 μ L, 0.78 mmol) was stirred at room temperature in CH₃CN (30 mL) for 12 hours. After filtration over Celite and evaporation of the solvent under vacuum, complexes [8](OTf) and [9](OTf)₂ were obtained as a pale yellow powder (ratio [8](OTf)/[9](OTf)₂: 9/1). After recrystallization from CH₃CN/Et₂O at -20 °C, [8](OTf) was isolated in a pure form as pale yellow crystals suitable for X-ray diffraction (0.16 g, 75%). ³¹P{¹H} NMR (162 MHz, CD₃CN, 25 °C): δ = 23.6 (s); ¹H NMR (400 MHz, CD₃CN, 25 °C) δ = 8.90–8.82 (m, 2H, H_{Py}), 7.99 (tt, J_{HH} = 7.6, 1.7 Hz, 1H, H_{Py}), 7.83–7.69 (m, 9H, H_{Ar}), 7.66–7.60 (m, 7H, H_{Ar}), 7.58–7.51 (m, 2H, H_{Py}), 7.41 (d, J_{HH} = 8.2 Hz, 1H, H_{Ar}), 7.31 (d, J_{HH} = 2.1 Hz, 1H, H_{Ar}), 7.09 (t, J_{HH} = 7.4 Hz, 1H, H_{Ar}), 7.00 (d, J_{HH} = 8.2 Hz, 1H, H_{Ar}), 6.75 (t, J_{HH} = 7.7 Hz, 1H, H_{Ar}), 4.77 (t, J_{HH} = 7.1 Hz, 2H, NCH₂), 3.59–3.43 (m, 2H, PCH₂), 2.55–2.38 (m, 2H, CH₂). ¹³C{¹H} NMR (101 MHz, CD₃CN, 25 °C): δ = 159.4 (s, N₂C), 150.4 (s, CH_{Py}), 148.6 (s, C_{Ph}), 140.1 (s, CH_{Py}), 136.1 (d, J_{CP} = 3.0 Hz, CH_{Ph}), 134.7 (d, J_{CP} = 10.6 Hz, CH_{Ph}), 132.0 (s, C_{Ph}), 131.2 (d, J_{CP} = 12.8 Hz, CH_{Ph}), 129.3 (s, CH_{Ph}), 126.1 (s, CH_{Ph}), 125.9 (s, CH_{Py}), 121.3 (s, CH_{Ph}), 120.8 (s, CH_{Ph}), 120.7 (q, J_{CF} = 319.9 Hz, CF₃), 120.3 (s, CH_{Im}), 118.9 (d, J_{CP} = 86.8 Hz, C_{Ph}), 117.0 (s, CH_{Im}), 50.6 (d, J_{CP} = 21.1 Hz, NCH₂), 25.4 (d, J_{CP} = 3.0 Hz, CH₂), 20.4 (d, J_{CP} = 54.4 Hz, PCH₂); MS (ES⁺): m/z : 684.1 [M - CF₃SO₃]⁺; elemental analysis for C₃₆H₃₂ClF₃N₃O₄PPdS.H₂O: calcd, C 50.84, H 4.03, N 4.94; found, C 50.59, H 3.75, N 4.77.

Synthesis of complex [9](OTf)₂

A mixture of [7](OTf)₂ (0.10 g, 0.13 mmol), PdCl₂ (0.011 g, 0.065 mmol), anhydrous K₂CO₃ (0.054 g, 0.39 mmol) was stirred at room temperature in CH₃CN (10 mL) for 12 hours. After filtration over Celite and evaporation of the solvent under vacuum, [9](OTf)₂ was obtained as a pale yellow powder (0.16 g, 92%). Recrystallization from CH₃CN/Et₂O at room temperature gave pale yellow crystals suitable for X-ray diffraction. ³¹P{¹H} NMR (162 MHz, CD₃CN, 25 °C): δ = 23.4 (s); ¹H NMR (400 MHz, CD₃CN, 25 °C) δ = 7.79–7.71 (m, 6H, H_{Ar}), 7.60–7.45 (m, 26H, H_{Ar}), 7.33–7.29 (m, 4H, H_{Ar}), 6.96 (t, J_{HH} = 7.4 Hz, 2H, H_{Ar}), 6.86 (d, J_{HH} = 8.2 Hz, 2H, H_{Ar}), 6.65 (t, J_{HH} = 7.7 Hz, 2H, H_{Ar}), 4.82 (t, J_{HH} = 7.1 Hz, 4H, NCH₂), 3.43–3.31 (m, 4H,

PCH₂), 2.40–2.27 (m, 4H, CH₂); ¹³C{¹H} NMR (101 MHz, CD₃CN, 25 °C): δ = 164.4 (s, N₂C), 159.0 (s, C_{Ph}), 136.0 (d, *J*_{CP} = 3.0 Hz, CH_{Ph}), 134.5 (d, *J*_{CP} = 10.6 Hz, CH_{Ph}), 131.2 (d, *J*_{CP} = 12.8 Hz, CH_{Ph}), 130.9 (s, C_{Ph}), 128.6 (s, CH_{Ph}), 125.3 (s, CH_{Ph}), 121.7 (s, CH_{Ph}), 121.4 (s, CH_{Ph}), 118.5 (d, *J*_{CP} = 86.8 Hz, C_{Ph}), 118.3 (s, CH_{Im}), 116.4 (s, CH_{Im}), 49.0 (d, *J*_{CP} = 21.1 Hz, NCH₂), 25.6 (d, *J*_{CP} = 3.0 Hz, CH₂), 20.6 (d, *J*_{CP} = 54.4 Hz, PCH₂); MS (ES⁺): *m/z*: 1179.2 [M – CF₃SO₃]⁺; HRMS (ES⁺): calcd for C₆₁H₅₄F₃N₄O₅P₂PdS, 1179.2297; found, 1179.2296.

Synthesis of complex **10**

1st method: [**8**](OTf) (0.04 g, 0.048 mmol) and anhydrous Cs₂CO₃ (0.078 g, 0.24 mmol) were dissolved in CH₃CN (15 mL), and the suspension was stirred at 70 °C for 12 hours. After filtration over Celite, the solvent was evaporated under vacuum. The crude residue was dissolved in CH₂Cl₂ (10 mL), and the solution was filtered over Celite. After evaporation of the solvent, **10** was obtained as a pale yellow powder (0.023 g, 85%).

2nd method: A mixture of [**7**](OTf)₂ (0.30 g, 0.39 mmol), PdCl₂ (0.07 g, 0.39 mmol), and anhydrous Cs₂CO₃ (0.63 g, 1.96 mmol) was stirred at 90 °C in CH₃CN (30 mL) for 12 hours. After filtration over Celite and evaporation of the solvent under vacuum, the crude residue was dissolved in CH₂Cl₂ (10 mL), and the solution was filtered over Celite. After evaporation of the solvent, **10** was obtained as a pale yellow powder (0.19 g, 84%). Recrystallization from a saturated CH₃CN solution at room temperature gave **10** as pale yellow crystals suitable for X-ray diffraction. ³¹P{¹H} NMR (162 MHz, CD₂Cl₂, 25 °C): δ = 33.8 (s); ¹H NMR (400 MHz, CD₂Cl₂, 25 °C) δ = 8.27 (brd, *J*_{HH} = 8.2 Hz, 1H, H_{Ar}), 7.75–7.50 (m, 10H, H_{Ar}), 7.45–7.35 (m, 4H, H_{Ar}), 7.25 (brd, *J*_{HH} = 8.2 Hz, 1H, H_{Ar}), 7.08 (brt, *J*_{HH} = 7.4 Hz, 1H, H_{Ar}), 7.02 (brt, *J*_{HH} = 7.4 Hz, 1H, H_{Ar}), 6.94 (brs, 1H, H_{Ar}), 6.44 (brt, *J*_{HH} = 7.7 Hz, 1H, H_{Ar}), 4.10–4.05 (m, 2H, NCH₂), 3.21–3.14 (m, 1H, PCH), 2.25–2.19 (m, 1H, CH₂), 2.00–1.89 (m, 1H, CH₂); ¹³C{¹H} NMR (101 MHz, CD₃CN, 25 °C): δ = 182.2 (d, *J*_{CP} = 37.2 Hz, C_{Ph-ortho}), 176.2 (d, *J*_{CP} = 7.0 Hz, C_{Ph}), 160.3 (s, N₂C), 150.7 (s, CH_{Ph}), 137.1 (d, *J*_{CP} = 119.7 Hz, C_{Ph-ipso}), 136.3 (d, *J*_{CP} = 19.1 Hz, CH_{Ph}), 135.0 (d, *J*_{CP} = 9.0 Hz, CH_{Ph}), 134.4 (d, *J*_{CP} = 10.1 Hz, CH_{Ph}), 133.8 (d, *J*_{CP} = 3.0 Hz, CH_{Ph}), 133.7 (d, *J*_{CP} = 8.0 Hz, CH_{Ph}), 133.4 (d, *J*_{CP} = 3.0 Hz, CH_{Ph}), 131.4 (d, *J*_{CP} = 13.1 Hz, CH_{Ph}), 130.5 (d, *J*_{CP} = 10.1 Hz, CH_{Ph}), 130.1 (d, *J*_{CP} = 3.0 Hz, CH_{Ph}), 129.8 (d, *J*_{CP} = 20.1 Hz, CH_{Ph}), 129.7 (d, *J*_{CP} = 11.1 Hz, CH_{Ph}), 128.3 (s, C_{Ph}), 127.7 (s, CH_{Ph}), 127.4 (d, *J*_{CP} = 85.5 Hz, C_{Ph}), 127.0 (d, *J*_{CP} = 54.3 Hz, C_{Ph}), 125.5 (d, *J*_{CP} = 10.1 Hz, CH_{Ph}), 124.8 (brs, CH_{Ph}), 124.2 (s, CH_{Ph}), 122.4 (s, CH_{Ph}), 122.1 (q, *J*_{CF} = 319.9 Hz, CF₃), 120.4 (s, CH_{Ph}), 116.7 (s, CH_{Im}), 112.8 (s, CH_{Im}), 52.7 (d, *J*_{CP} = 22.1 Hz, NCH₂), 27.4 (s, CH₂), 13.8 (d, *J*_{CP} = 40.2 Hz, PCH); MS (ES⁺): *m/z*: 567.1 [MH⁺]; HRMS (ES⁺): calcd for C₃₀H₂₆N₂OPPd,

567.0829; found, 567.0833. elemental analysis for $C_{30}H_{25}N_2OPPd \cdot 1.2CH_2Cl_2$: calcd, C 56.03, H 4.13, N 4.19; found, C 55.55, H 3.94, N 4.77.

Synthesis of complex [11a](OTf)

TfOH (0.5 M in CH_3CN , 158 μ L, 0.079 mmol) was added at -40 $^{\circ}C$ to a solution of complex **10** (0.045 g, 0.079 mmol) in CH_3CN (10 mL). The mixture was warmed to room temperature for 2 hours. After filtration over Celite, the solvent was removed under vacuum, and complex [11a](OTf) was obtained as a pale yellow powder (0.056 g, 94%). $^{31}P\{^1H\}$ NMR (162 MHz, CD_3CN , 25 $^{\circ}C$): δ = 29.0 (s); 1H NMR (400 MHz, CD_3CN , 25 $^{\circ}C$) δ = 7.85–7.80 (m, 5H, H_{Ar}), 7.67–7.63 (m, 3H, H_{Ar}), 7.51–7.43 (m, 8H, H_{Ar}), 7.33 (d, J_{HH} = 8.2 Hz, 1H, H_{Ar}), 7.05 (t, J_{HH} = 7.4 Hz, 1H, H_{Ar}), 6.93 (brs, 1H, H_{Ar}), 6.76 (d, J_{HH} = 8.2, Hz, 1H, H_{Ar}), 6.62 (t, J_{HH} = 7.7 Hz, 1H, H_{Ar}), 4.02–3.95 (m, 1H, NCH_2), 3.84–3.78 (m, 1H, NCH_2), 3.73–3.68 (m, 1H, PCH), 2.60–2.50 (m, 1H, CH_2), 2.15–2.05 (m, 1H, CH_2); $^{13}C\{^1H\}$ NMR (101 MHz, CD_3CN , 25 $^{\circ}C$): δ = 158.8 (s, N_2C), 152.4 (s, C_{Ph}), 134.7 (d, J_{CP} = 10.6 Hz, CH_{Ph}), 134.5 (d, J_{CP} = 3.0 Hz, CH_{Ph}), 130.3 (d, J_{CP} = 12.8 Hz, CH_{Ph}), 128.9 (s, CH_{Ph}), 127.8 (s, C_{Ph}), 123.8 (d, J_{CP} = 86.8 Hz, C_{Ph}), 123.3 (s, CH_{Ph}), 122.7 (q, J_{CF} = 320.9 Hz, CF_3), 121.8 (s, CH_{Ph}), 121.0 (s, CH_{Ph}), 119.3 (s, CH_{Im}), 114.8 (s, CH_{Im}), 50.9 (d, J_{CP} = 21.1 Hz, NCH_2), 26.7 (s, CH_2), 5.7 (d, J_{CP} = 32.2 Hz, PCH); MS (ES^+): m/z : 567.1 [$M - CH_3CN - CF_3SO_3$] $^+$; HRMS (ES^+): calcd for $C_{30}H_{26}N_2OPPd$, 567.0829; found, 567.0859.

Synthesis of complex [11b](OTf)

t-butyl isocyanide (6.87 μ L, 0.059 mmol) was added at -78 $^{\circ}C$ to a solution of complex [11a](OTf) (0.03 g, 0.039 mmol) in CH_2Cl_2 (10 mL). The mixture was warmed to room temperature for 2 hours. After filtration over Celite, the solvent was removed under vacuum, and complex [11b](OTf) was obtained as a pale yellow powder (0.03 g, 95 %). $^{31}P\{^1H\}$ NMR (162 MHz, CD_2Cl_2 , 25 $^{\circ}C$): δ = 31.8 (s); 1H NMR (400 MHz, CD_2Cl_2 , 25 $^{\circ}C$) δ = 7.89–7.84 (m, 5H, H_{Ar}), 7.72–7.68 (m, 5H, H_{Ar}), 7.58–7.54 (m, 5H, H_{Ar}), 7.47 (brs, 1H, H_{Ar}), 7.28–7.25 (m, 1H, H_{Ar}), 7.13–7.09 (m, 1H, H_{Ar}), 7.05 (brs, 1H, H_{Ar}), 6.90 (d, J = 8.2, Hz, 1H, H_{Ar}), 6.65 (t, J_{HH} = 7.7 Hz, 1H, H_{Ar}), 4.09–4.05 (m, 2H, NCH_2), 3.36–3.29 (m, 1H, PCH), 2.38–2.30 (m, 1H, CH_2), 1.57–1.41 (m, 1H, CH_2), 1.18 (s, 9H, *t*Bu); $^{13}C\{^1H\}$ NMR (101 MHz, CD_2Cl_2 , 25 $^{\circ}C$): δ = 158.2 (s, N_2C), 158.0 (s, C_{Ph}), 134.5 (d, J_{CP} = 3.0 Hz, CH_{Ph}), 134.3 (d, J_{CP} = 10.6 Hz, CH_{Ph}), 130.3 (d, J_{CP} = 12.8 Hz, CH_{Ph}), 128.4 (s, CH_{Ph}), 125.0 (s, C_{Ph}), 123.2 (d, J_{CP} = 82.5 Hz, C_{Ph}), 122.7 (s, CH_{Ph}), 122.4 (s, CH_{Ph}), 121.3 (q, J_{CF} = 320.9 Hz, CF_3), 120.2 (s, CH_{Ph}), 118.7 (s, CH_{Im}), 114.8 (s, CH_{Im}), 58.4 (s, $C(CH_3)_3$), 51.0 (d, J_{CP} = 21.1 Hz, NCH_2), 30.0 (s, CH_3), 27.0 (s, CH_2), 3.3 (d, J_{CP} = 32.7 Hz, PCH); MS (ES^+): m/z : 567.1 [$M - tBuNC$

– CF₃SO₃]⁺; HRMS (ES⁺): calcd for C₃₀H₂₆N₂OPPd, 567.0829; found, 567.0842. * The ¹³C NMR resonance of the CN quaternary carbon atom of coordinated *t*-BuNC was not observed.

Palladium-Catalyzed Allylation of Aldehydes by Pincer Complexes: Representative procedure for the allylation of benzaldehyde with allyltributyltin in the presence of palladium complex [12a](OTf)₂.

To a mixture of benzaldehyde (27 mg, 26 μl, 0.25 mmol) and Pd complex [12a](OTf)₂ (14 mg, 0.0127 mmol, 5.0 mol %) in DMF (0.6 mL) was added allyltributyltin (94 μl, 0.30 mmol) under nitrogen. The solution was stirred at 60 °C for 18 hours. The reaction mixture was then quenched with water and the product was extracted with diethyl ether (3 x 5 mL). The combined organic phases were dried over Na₂SO₄ and concentrated. The crude residue was purified by chromatography on silica gel with pentane/EtOAc (9/1 to 8/2) to afford the homoallylic alcohol as colorless oil (28 mg, 75%). The ¹H and ¹³C NMR data obtained are in agreement with the corresponding literature.³⁷

Single-crystal X-ray diffraction analyses

Intensity data of [4](OTf), [7]Br₂, [8](OTf), [9](OTf)₂, and 10 were collected at low temperature on an Apex2 Bruker equipped with a 30W air-cooled microfocus Mo source (λ = 0.71073 Å). The structures were solved using SUPERFLIP,³⁸ and refined by means of least-squares procedures using CRYSTALS.³⁹ Atomic scattering factors were taken from the international tables for X-ray crystallography. All non-hydrogen atoms were refined anisotropically. Hydrogen atoms were refined using a riding model. Absorption corrections were introduced using the program MULTISCAN.⁴⁰

Electrochemistry data

Voltammetric measurements were carried out with a potentiostat Autolab PGSTAT100 on Pd complexes [4a](OTf), [5a](OTf)₂, 10, and [11a](OTf). Experiments were performed at room temperature in an homemade airtight three-electrode cell connected to a vacuum/argon line. The reference electrode consisted of a saturated calomel electrode (SCE) separated from the solution by a bridge compartment. The counter electrode was a platinum wire of *ca* 1 cm² apparent surface. The working electrode was a Pt microdisk (0.5 mm diameter). Voltammograms were recorded in dry CH₃CN solution (≈ 10⁻³ M) in the presence of 0.1 M *n*-tetrabutylammonium triflate as the supporting electrolyte, under nitrogen at 25 °C. In reference 14, the value of +2.00 V given for the oxidation of complex [12a](OTf)₂ corresponds to its second oxidation potential.

Computational details

Geometries were fully optimized at the PBE-D3/6-31G**/LANL2DZ* (Pd) level of calculation using Gaussian 09.⁴¹ The star in LANL2DZ*(Pd) refers to *f*-polarization functions derived by Ehlers *et al.*⁴² for Pd, that have been added to the LANL2DZ(Pd) basis set. Vibrational analysis was performed at the same level as the geometry optimization in order to check the obtention of a minimum on the potential energy surface. Gibbs free energies were calculated at 298.15 K. Electron Localization Function (ELF) analysis and Quantum Theory of Atoms in Molecules (QTAIM)⁴³ topological analyses were performed with the TopMoD package.⁴⁴ The topological analysis of the electron density yields a partition of the molecular space into atomic basins. The topological analysis of the ELF gradient field yields a partition of the molecular space into non-overlapping electronic domains, classified into core, valence bonding and nonbonding basins.⁴⁵⁻⁴⁸ These basins are in one-to-one correspondence to the core, lone or shared pairs of the Lewis model. A core basin contains a nucleus X (except a proton) and is designated as C(X). A valence bonding basin referred to as V(X,Y, ..) lies between two or more core basins. Among chemical reactivity descriptors of the “conceptual DFT”, Fukui functions are suitable for probing soft sites of reactants that are involved in orbital-controlled interactions with electrophiles, nucleophiles or radicals. The Fukui function was introduced by Parr and Yang as the response of the electron density of the molecular system to a change in the global number of electrons.⁴⁹ It can be expressed as the derivative of the electron density $\rho(r)$ with respect to the number of electrons N, calculated at a constant external potential $v(r)$.

In this work, frontier molecular orbital (FMO) Fukui functions (in which the electron density is approximated by densities of the FMOs) condensed within QTAIM⁵⁰ or ELF⁵¹ topological partitions have been used. $f_X^\square(r) = \int_X |\square_{KS}^F(r)|^2 dr$ is therefore the contribution of the FMO F ($\square = -$: F = HOMO ; $\square = +$: F = LUMO) to the atomic QTAIM basin or to the core or valence ELF basin X. These Fukui indices are confined into the 0-1 range and they sum up to one: $0 \leq f_X^\square \leq 1$ et $\sum_X f_X^\square = 1$. The larger the value of the *f* index, the more reactive the corresponding basin X.

Supporting Information

The supporting Information of this article can be found under <https://...>

- ³¹P, ¹H and ¹³C NMR spectra for all new compounds,
- Crystallographic table for [4](OTf), [7]Br₂, [8](OTf), [9](OTf)₂, and 10,
- Optimized structures of pincer Pd complexes 7²⁺, 11⁺, 12²⁺ and 13⁺.

Author Information

Corresponding author: *E-mail for Y.C.: yves.canac@lcc-toulouse.fr.

ORCID

Yves Canac: 0000-0002-3747-554X

Christine Lepetit: 0000-0002-0008-9506

Dmitry A. Valyaev: 0000-0002-1772-844X

Notes

The authors declare no competing financial interests

Acknowledgements

The authors thank the Centre National de la Recherche Scientifique for financial support, and Alix Saquet for electrochemistry experiments. R. T. is grateful to French MENESR for a PhD fellowship. The Mitacs program is also thanked for a research grant for A. G. Computational studies were performed using HPC resources from CALMIP (Grant 2019 [0851]) and from GENCI-[CINES/IDRIS] (Grant 2019 [085008]).

REFERENCES

- (1) (a) Igau, A.; Grützmacher, H.; Baceiredo, A.; Bertrand, G. Analogous α,α' -bis-carbenoid triply bonded species: synthesis of stable λ^3 -phosphinocarbene- λ^5 -phosphinoacetylene. *J. Am. Chem. Soc.* **1988**, *110*, 6463–6466. (b) Arduengo III, A. J.; Harlow, R. L.; Kline, M. A stable crystalline carbene. *J. Am. Chem. Soc.* **1991**, *113*, 361–363.
- (2) (a) Bourissou, D.; Guerret, O.; Gabbai, F. P.; Bertrand, G. Stable carbenes. *Chem. Rev.* **2000**, *100*, 39–91. (b) Y. Canac, M. Soleilhavoup, S. Conejero, G. Bertrand, Stable non-N-heterocyclic carbenes (non-NHC): recent progress. *J. Organomet. Chem.* **2004**, *689*, 3857–3865. (c) Hahn, F. E.; Jahnke, M. C. Heterocyclic carbenes: synthesis and coordination chemistry. *Angew. Chem. Int. Ed.* **2008**, *47*, 3122–3172. (d) Melaimi, M.; Soleilhavoup, M.; G. Bertrand, G. Stable carbenes and related species beyond diaminocarbenes. *Angew. Chem. Int. Ed.* **2010**, *49*, 8810–8849. (e) Benhamou, L.; Chardon, E.; Lavigne, G.; Bellemin-Laponnaz.; César, V. Synthetic routes to N-Heterocyclic carbenes. *Chem. Rev.* **2011**, *111*, 2705–2733. (f) Nelson, D. J.; Nolan, S. P. Quantifying and understanding the electronic properties of N-Heterocyclic carbenes. *Chem. Soc. Rev.* **2013**, *42*, 6723–6753. (g) Hopkinson, M. N.; Richter, C.; Schedler, M.; Glorius, F. An overview of N-Heterocyclic carbenes. *Nature* **2014**, *510*, 485–496.

(3) Abel, E. W.; Stone, F. G. A; Wilkinson, G. *Comprehensive Organometallic Chemistry II*, Vols. 7–9, Pergamon, New York, **1995**.

(4) (a) Schmidbaur, H. Phosphorus ylides in the coordination sphere of transition metals: an inventory. *Angew. Chem. Int. Ed. Engl.* **1983**, *22*, 907–927. (b) Kaska, W. C.; Ostoja Starzewski, K. A, in: *Ylides and Imines of Phosphorus*; Johnson, A. W., Eds, John Wiley & Sons: New York, **1993**, chapt. 14. (c) Kolodiazhnyi, O. I. C-element-substituted phosphorus ylides. *Tetrahedron* **1996**, *52*, 1855–1929. (d) Vicente, J. Chicote, M. T. The ‘acac method’ for the synthesis and coordination of organometallic compounds: synthesis of gold complexes. *Coord. Chem. Rev.* **1999**, *193-195*, 1143–1161. (e) Falvello, L. R. ; Ginés, J. C.; Carbó, J. J.; Lledós, A.; Navarro, R.; Soler, T.; Urriolabeitia, E. P. Palladium complexes of a phosphorus ylide with two stabilizing groups: synthesis, structure, and DFT study of the bonding modes. *Inorg. Chem.* **2006**, *45*, 6803–6815. (f) Urriolabeitia, E. P. *sp*³-hybridized neutral η^1 -carbon ligands. *Top. Organomet. Chem.* Chauvin, R.; Canac, Y. Eds, Springer, **2010**, *30*, 15–48.

(5) (a) Scherpf, T.; Feichtner, K. S.; Gessner, V. H. Using ylide functionalization to stabilize boron cations. *Angew. Chem. Int. Ed.* **2017**, *56*, 3275–3279. (b) Scharf, L. T.; Gessner, V. H. Metalated ylides: a new class of strong donor ligands with unique electronic properties. *Inorg. Chem.* **2017**, *56*, 8599–8607. (c) Mohapatra, C.; Scharf, L.; Scherpf, T.; Mallick, B.; Feichtner, K-S.; Schwarz, C.; Gessner, V. H. Isolation of a diylide-stabilized stannylene and germylene: enhanced donor strength coplanar lone pair alignment. *Angew. Chem. Int. Ed.* **2019**, *58*, 7459–7463.

(6) (a) Maaliki, C.; Abdalilah, M.; Barthes, C.; Duhayon, C.; Canac, Y.; Chauvin, R. Bis-ylide ligands from acyclic proximal diphosphonium precursors. *Eur. J. Inorg. Chem.* **2012**, 4057–4064. (b) Serrano, E.; Soler, T.; Urriolabeitia, E. P. Regioselective C-H bond activation of asymmetric bis(ylide)s promoted by Pd. *Eur. J. Inorg. Chem.* **2017**, 2220–2230. (c) Scherpf, T.; Schwarz, C.; Scharf, L. T.; Zur, J-A.; Helbig, A.; Gessner, V. H. Ylide-functionalized phosphines: strong donor ligands for homogeneous catalysis. *Angew. Chem. Int. Ed.* **2018**, *57*, 12859–12864. (d) Weber, P.; Scherpf, T.; Rodstein, I.; Lichte, D.; Scharf, L. T.; Gooßen, L. J.; Gessner, V. H. A highly active ylide-functionalized phosphine for palladium catalyzed aminations of aryl chlorides. *Angew. Chem. Int. Ed.* **2019**, *58*, 3203–3207. (e) Scherpf, T.; Rodstein, I.; Paaßen, M.; Gessner, V. H. Group 9 and 10 metal complexes of an ylide-substituted phosphine : coordination versus cyclometalation and oxidative addition. *Inorg. Chem.* **2019**, *58*, 8151–8161.

-
- (7) Canac, Y.; Lepetit, C.; Abdalilah, M.; Duhayon, C.; Chauvin, R. Diaminocarbene and phosphonium ylide ligands: a systematic comparison of their donor character. *J. Am. Chem. Soc.* **2008**, *130*, 8406–8413.
- (8) Canac, Y.; Lepetit, C. Classification of the electronic properties of chelating ligands in *cis*-[LL’Rh(CO)₂] complexes. *Inorg. Chem.* **2017**, *56*, 667–675.
- (9) (a) Díez-González, S.; Marion, N.; Nolan, S. P. N-heterocyclic carbenes in late transition metal catalysis. *Chem. Rev.* **2009**, *109*, 3612–3676. (b) Riener, K.; Haslinger, S.; Raba, A.; Högerl, M. P.; Cokoja, M.; Herrmann, W. A.; Kühn, F. E. Chemistry of iron N-heterocyclic carbene complexes: syntheses, structures, reactivities, and catalytic applications. *Chem. Rev.* **2014**, *114*, 5215–5272.
- (10) Chauvin, R.; Canac, Y. Eds. Late transition metals of neutral η^1 -carbon ligands. *Top. Organomet. Chem.* Vol. 30 ; Springer: Berlin, Heidelberg, Germany, 2010; pp 1–252.
- (11) (a) Canac, Y.; Duhayon, C.; Chauvin, R. A diaminocarbene-phosphonium ylide: direct access to C,C-chelating ligands. *Angew. Chem. Int. Ed.* **2007**, *46*, 6313–6315. (b) Abdallah, I.; Debono, N.; Canac, Y.; Duhayon, C.; Chauvin, R. Atropochiral (C,C)-chelating NHC-ylide ligands: synthesis and resolution of palladium(II) complexes thereof. *Dalton Trans.* **2009**, 7196–7202. (c) Canac, Y.; Chauvin, R. Atropochiral C,X- and C,C-chelating carbon ligands. *Eur. J. Inorg. Chem.* **2010**, 2325–2335.
- (12) Benaissa, I.; Taakili, R.; Lugan, N.; Canac, Y. A convenient access to N-phosphonio-substituted NHC metal complexes [M = Ag(I), Rh(I), Pd(II)]. *Dalton Trans.* **2017**, *46*, 12293–12305.
- (13) Barthes, C.; Bijani, C.; Lugan, N.; Canac, Y. A palladium(II) complex of a C₄ chelating bis(NHC) diphosphonium bis(ylide) ligand. *Organometallics* **2018**, *37*, 673–678.
- (14) Taakili, R.; Lepetit, C.; Duhayon, C.; Valyaev, D. A.; Lugan, N.; Canac, Y. Palladium(II) pincer complexes of a C,C,C-NHC, diphosphonium bis(ylide) ligand. *Dalton Trans.* **2019**, *48*, 1709–1721.
- (15) Canac, Y. Carbeniophosphines versus phosphoniocarbenes: the role of the positive charge. *Chem. Asian. J.* **2018**, *13*, 1872–1887.
- (16) (a) Bolliger, J. L.; Blacque, O.; Frech, C. M. Short, facile, and high-yielding synthesis of extremely efficient pincer-type Suzuki catalysts bearing aminophosphine substituents. *Angew. Chem. Int. Ed.* **2007**, *46*, 6514–6517. (b) Lisena, J.; Monot, J.; Mallet-Ladeira, S.; Martin-Vaca, B.; Bourissou, D. Influence of the ligand backbone in pincer complexes: indenediide-, indolyl-, and indenyl-based SCS palladium complexes. *Organometallics* **2013**, *32*, 4301–4305.

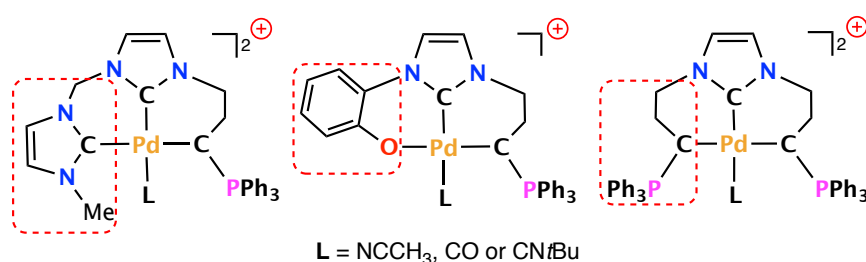
-
- (17) Green, M. L. H. A new approach to the formal classification of the covalent compounds of the elements. *J. Organomet. Chem.* **1995**, *500*, 127–148.
- (18) (a) van Koten, G. Tuning the reactivity of metals held in a rigid ligand environment. *Pure Appl. Chem.* **1989**, *61*, 1681–1694. (b) Benito-Garagorri, D.; Kirchner, K. Modularly designed transition metal PNP and PCP pincer complexes based on aminophosphines: synthesis and catalytic applications. *Acc. Chem. Res.* **2008**, *41*, 201–203. (c) Roddick, D. M.; Zargarian, D. Pentacoordination for pincer and related terdentate coordination compounds: revisiting structural properties and trends for d⁸ transition metal systems. *Inorg. Chim. Acta* **2014**, *422*, 251–264.
- (19) (a) Chianese, A. R.; Li, X.; Janzen, M. C.; Faller, J. W.; Crabtree, R. H. Rhodium and iridium complexes of N-heterocyclic carbenes via transmetalation: structures and dynamics. *Organometallics* **2003**, *22*, 1663–1667. (b) Chaquin, P.; Canac, Y.; Lepetit, C.; Zargarian, D.; Chauvin, R. Estimating local bonding/antibonding character of canonical molecular orbitals from their energy derivatives. The case of coordinating lone pairs. *Int. J. Quantum Chem.* **2016**, *116*, 1285–1295.
- (20) Weiss, D. T.; Haslinger, S.; Jandl, C.; Pöthig, A.; Cokoja, M.; Kühn, F. E. Application of open chain tetraimidazolium salts as precursors for the synthesis of silver tetra(NHC) complexes. *Inorg. Chem.* **2015**, *54*, 415–417.
- (21) Grim, S. O.; Davidoff, E. F.; Marks, T. J. Preparation and ³¹P chemical shifts of some quaternary phosphonium salts. *Z. Naturforsch. B: Anorg. Chem. Org. Chem. Biochem. Biophys. Biol.* **1971**, *26*, 184–190.
- (22) Imidazolium and phosphonium derivatives are generally characterized by pK_a values between 20 and 24 in DMSO. For pK_a values, see: http://evans.rc.fas.harvard.edu/pdf/evans_pka_table.pdf.
- (23) The addition of an equiv. of base such as KHMDS results in the partial conversion of NHC Pd complex with the formation of a mixture of corresponding pincer and *ortho*-metallated complexes.
- (24) (a) Delis, J. G. P.; Aubel, P. G.; Vrieze, K.; van Leeuwen, P. W. N. M. Isocyanide insertion into the palladium-carbon bond of complexes containing bidentate nitrogen ligands: a structural and mechanistic study. *Organometallics* **1997**, *16*, 2948–2957. (b) Badaj, A. C.; Lavoie, G. G. Reactivity study of imino-N-heterocyclic carbene palladium methyl complexes. *Organometallics* **2013**, *32*, 4577–4590.
- (25) The IR ν_{CN} frequency of free *t*-BuNC is observed at 2139 cm⁻¹ in CH₂Cl₂.

-
- (26) Pratt, D. A.; Pesavento, R. P.; van der Donk, W. A. Synthesis and pK_a determination of 1-(*o*-hydroxyphenyl)imidazole carboxylic esters. *J. Chem. Soc. Perkin Trans 1*, **2000**, 1217–1221.
- (27) O'Brien, C. J.; Kantchev, E. A. B.; Valente, C.; Hadei, N.; Chass, G. A.; Lough, A.; Hopkinson, A. C.; Organ, M. G. Easily prepared air- and moisture-stable Pd NHC (NHC = N-heterocyclic carbene) complexes: a reliable, user-friendly, highly active palladium precatalyst for the Suzuki-Miyaura reaction. *Chem. Eur. J.* **2006**, *12*, 4743–4748.
- (28) CCDC 1981606 [4](OTf), CCDC 1981607 [7]Br₂, CCDC 1981608 [8](OTf), CCDC 1981609 [9](OTf)₂, and CCDC 1981610 **10** contain the supplementary crystallographic data for this paper. These data can be obtained free of charge from the Cambridge Crystallographic Data Centre via www.ccdc.cam.ac.uk/data_request/cif.
- (29) Yang, L.; Powell, D. R.; Houser, R. P. Structural variation in copper(I) complexes with pyridylmethylamide ligands: structural analysis with a four-coordinate geometry index, τ_4 . *Dalton Trans.* **2007**, 955–964.
- (30) The calculation level was validated by a reasonable agreement between optimized geometries and the available X-ray crystal structure of Pd complex [12b](OTf)₂.¹⁴
- (31) The optimized geometries of Pd pincer complexes **5**²⁺, **11**⁺, **12**²⁺ (with L = CN*t*Bu and CO), and **13**⁺ calculated at the PBE-D3/6-31G**/LANL2DZ*(Pd) level are given in the supplementary information (Fig. S39-S42). For L = NCCH₃, see reference 14.
- (32) Selander, N.; Szabó, K. J. Catalysis by palladium pincer complexes. *Chem. Rev.* **2011**, *111*, 2048–2076.
- (33) (a) Solin, N.; Kjellgren, Szabó, K. J. Palladium-catalyzed electrophilic substitution via monoallylpalladium intermediates. *Angew. Chem. Int. Ed. Engl.* **2003**, *42*, 3656–3658. (b) Solin, N.; Kjellgren, J.; Szabó, K. J. Pincer complex-catalyzed allylation of aldehyde and imine substrates via nucleophilic η^1 -allyl palladium intermediates. *J. Am. Chem. Soc.* **2004**, *126*, 7026–7033.
- (34) During all the catalytic tests, no formation of insoluble black precipitate was observed which could suggest the formation of catalytically active Pd(0) nanoparticles.
- (35) (a) Gründemann, S.; Albrecht, M.; Loch, J. A.; Faller, J. W.; Crabtree, R. H. Tridentate carbene CCC and CNC pincer palladium(II) complexes: structure, fluxionality, and catalytic activity. *Organometallics* **2001**, *20*, 5485–5488. (b) Barzack, N. T.; Grote, R. E.; Jarvo, E. R. Catalytic umpolung allylation of aldehydes by π -allylpalladium complexes containing bidentate N-heterocyclic carbene ligands. *Organometallics* **2007**, *26*, 4863–4865.

-
- (36) It is well-known that Pd(II) species readily undergo transmetallation with allylstannanes to form allylpalladium complexes, see: Nakamura, H.; Iwama, H.; Yamamoto, Y. Palladium- and platinum-catalyzed addition of aldehydes and imines with allylstannanes. Chemoselective allylation of imines in the presence of aldehydes. *J. Am. Chem. Soc.* **1996**, *118*, 6641–6647.
- (37) (a) Yao, Q.; Sheets, M. A SeCSe–Pd(II) pincer complex as a highly efficient catalyst for allylation of aldehydes with allyltributyltin. *J. Org. Chem.* **2006**, *71*, 5384–5387. (b) Piechaczyk, O.; Cantat, T.; Mézailles, N.; Le Floch, P. A joint experimental and theoretical study of the palladium-catalyzed electrophilic allylation of aldehydes. *J. Org. Chem.* **2007**, *72*, 4228–4237.
- (38) Palatinus, L.; Chapuis, G. Superflip – a computer program for the solution of crystal structures by charge flipping in arbitrary dimensions. *J. Appl. Cryst.* **2007**, *40*, 786–790.
- (39) Betteridge, P. W.; Carruthers, J. R.; Cooper, R. I.; Prout, K.; Watkin, D. J. Crystals version 12: software for guided crystal structure analysis. *J. Appl. Cryst.* **2003**, *36*, 1487.
- (40) Blessing, R. H. An empirical correction for absorption anisotropy. *Acta Crystallogr.* **1995**, *A51*, 33–38.
- (41) Gaussian 09, Revision D.01, Frisch, M. J.; Trucks, G. W.; Schlegel, H. B.; Scuseria, G. E.; Robb, M. A.; Cheeseman, J. R.; Scalmani, G.; Barone, V.; Mennucci, B.; Petersson, G. A.; Nakatsuji, H.; Caricato, M.; Li, X.; Hratchian, H. P.; Izmaylov, A. F.; Bloino, J.; Zheng, G.; Sonnenberg, J. L.; Hada, M.; Ehara, M.; Toyota, K.; Fukuda, R.; Hasegawa, J.; Ishida, M.; Nakajima, T.; Honda, Y.; Kitao, O.; Nakai, H.; Vreven, T.; Montgomery, J. A.; Peralta, J. E.; Ogliaro, F.; Bearpark, M.; Heyd, J. J.; Brothers, E.; Kudin, K. N.; Staroverov, V. N.; Kobayashi, R.; Normand, J.; Raghavachari, K.; Rendell, A.; Burant, J. C.; Iyengar, S. S.; Tomasi, J.; Cossi, M.; Rega, N.; Millam, J. M.; Klene, M.; Knox, J. E.; Cross, J. B.; Bakken, V.; Adamo, C.; Jaramillo, J.; Gomperts, R.; Stratmann, R. E.; Yazyev, O.; Austin, A. J.; Cammi, R.; Pomelli, C.; Ochterski, J. W.; Martin, R. L.; Morokuma, K.; Zakrzewski, V. G.; Voth, G. A.; Salvador, P.; Dannenberg, J. J.; Dapprich, S.; Daniels, A. D.; Farkas, Ö.; Foresman, J. B.; Ortiz, J. V.; Cioslowski, J.; Fox, D. J. Gaussian, Inc., Wallingford CT, 2009
- (42) Ehlers, A.W.; Böhme, M.; Dapprich, S.; Gobbi, A.; Höllwarth, A.; Jonas, V.; Köhler, K. F.; Stegmann, R.; Veldkamp, A.; Frenking, G. A set of f-polarization functions for pseudo-potential basis sets of the transition metals Sc-Cu, Y-Ag and La-Au. *Chem. Phys. Lett.* **1993**, *208*, 111–114.
- (43) Bader, R. F. W. in *Atoms In Molecules*; Clarendon Press: Oxford. UK. **1990**.
- (44) Noury, S.; Krokidis, X.; Fuster, F.; Silvi, B. Computational tools for the electron localization function topological analysis. *Comput. & Chem.* **1999**, *23*, 597–604.

- (45) Poater, J.; Duran, M.; Sola, M.; Silvi, B. Theoretical evaluation of electron delocalization in aromatic molecules by means of atoms in molecules (AIM) and electron localization function (ELF) topological approaches. *Chem. Rev.* **2005**, *105*, 3911–3947.
- (46) (a) Becke, A. D.; Edgecombe, K. E. A simple measure of electron localization in atomic and molecular systems. *J. Chem. Phys.* **1990**, *92*, 5397–5403. (b) Silvi, B.; Savin, A. Classification of chemical bonds based on topological analysis of electron localization functions. *Nature* **1994**, *371*, 683–686.
- (47) Silvi, B.; Furre, I.; Alikhani, M. E. The topological analysis of the electron localization function. A key for a position space representation of chemical bonds. *Monatshefte für Chemie* **2005**, *136*, 855–879.
- (48) Silvi, B.; Gillespie, R. J.; Gatti, C. in *Comprehensive Inorganic Chemistry II* **2013**, *9*, 187–226.
- (49) Parr, R. G.; Yang, W. Density functional approach to the frontier-electron theory of chemical reactivity. *J. Am. Chem. Soc.* **1984**, *106*, 4049–4050.
- (50) Bulat, F. A.; Chamorro, E.; Fuentealba, P.; Toro-Labbé, A. Condensation of frontier molecular orbital Fukui functions. *J. Phys. Chem.* **2004**, *108*, 342–349.
- (51) Tiznado, W.; Chamorro, E.; Contreras, R.; Fuentealba, P. Comparison among four different ways to condense the Fukui function. *J. Phys. Chem.* **2005**, *109*, 3220–3224.

For Table of contents only



The coordinating properties and catalytic performances of NHC, phenolate and phosphonium ylide donor moieties are evaluated through the preparation of an isostructural family of NHC core, phosphonium ylide-based palladium(II) pincer complexes.